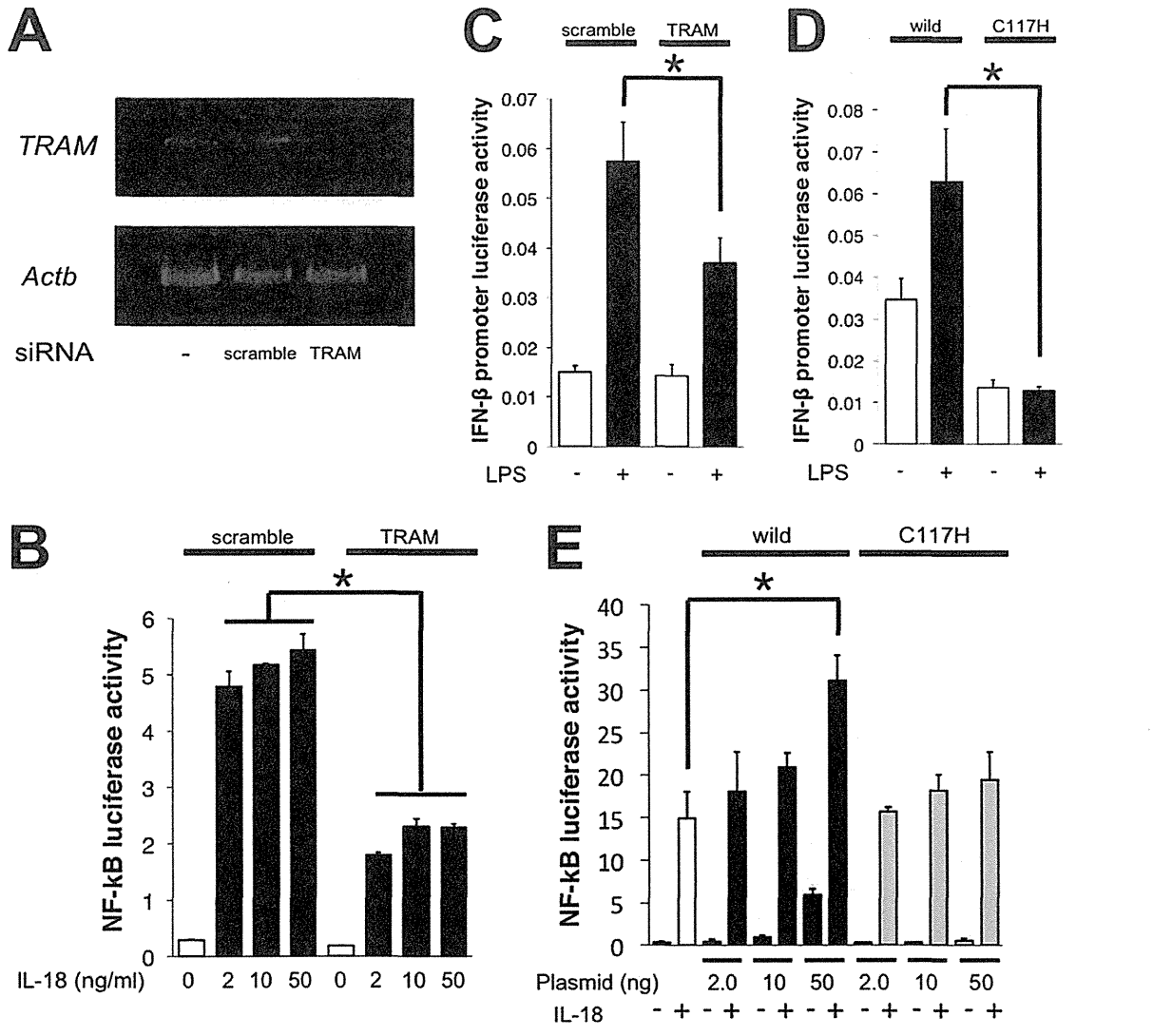

Figure 3. The knock-down effects of TRAM in IL-18 or LPS/TLR4 signaling. (A) RT-PCR of the *TRAM* mRNA knock-down in HEK293T cells by the psiRNA-TICAM-2 but not by the nonspecific scrambled sequence coded psiRNA vector. "-" indicates cells not transfected with siRNA; *"Actb"* indicates the loading control (β-actin mRNA). (B–E) The effect of the knock-down of TRAM using shRNA or the dominant negative form of TRAM (C117H) for the IL-18 or LPS induced NF-κB or IFN-β-promoter luciferase activity assay. The NF-κB and IFN-β-promoter activities with IL-18 or LPS stimulation were significantly decreased in the IL-18Rβ co-transfected HEK293T cells or HEK293-hTLR4-MD2-CD14 cells.
doi:10.1371/journal.pone.0038423.g003

the other hand, recent reports have shown that TRAM is associated not only with TLR4 but also with the TLR2 and TLR5 signaling pathways [23,24]. These findings suggest that the conventionally accepted definition of the functions of the TIR domain-containing adaptor proteins in the TLR and IL-1/18 signaling pathways should be reconsidered.

Time Dependent Change of the Interaction between MyD88 and TRAM

A particularly interesting feature we observed in this study was that the complex between Myc-MyD88 and FLAG-TRAM expressed in HEK293T cells decreased after IL-18 stimulation in a time-dependent manner (Figure 2). This observation suggests that either the rearrangement of the signal initiation complexes or the degradation of the components in the complexes is triggered by the activation of the IL-18 signaling. A similar rearrangement of the signal initiation complex has also been observed for the TLR4 pathway in a previous report; upon activation of TLR4 by LPS, TLR4 associated with MyD88 instantly, and the association was lost within 15 min [25]. Thus, such transient interactions between the receptors and adaptors and the subsequent loss of the interaction may be common to both the TLR and the IL-18 pathways especially because they utilize many of the same intracellular components. For the TLR4 complex, phosphorylation of TLR4 and Mal has been suggested to be involved in the rearrangements [25,26]. TRAM has been shown to be phosphorylated by Protein kinase C-ε (PKC-ε) upon stimulation by LPS, and the phosphorylation has been implicated in regulating the

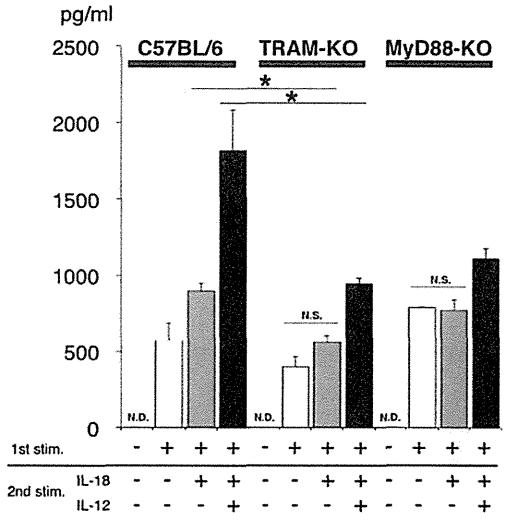

Figure 4. The IFN-γ production from IL-18 and/or IL-12 stimulated Th1 cells from TRAM-deficient mice and MyD88 deficient mice. The IFN-γ production levels were significantly reduced in TRAM deficient mice and MyD88 deficient mice. The black bars show the production levels from IL-18 and IL-12 co-stimulated Th1 cells, grey bars show those from IL-18 solely stimulated Th1 cells, and the white bars show those from no secondary stimulated Th1 cells.
doi:10.1371/journal.pone.0038423.g004

myristoylation state and thus the membrane targeting [10,27]. The membrane targeting of another myristoylated protein, MARCKS, has been shown to be regulated by phosphorylation; MARCKS is released from the plasma membrane upon the PKC mediated phosphorylation of a serine near its myristoylation site [28]. Similar to these examples, TRAM might be phosphorylated in the IL-18-induced dissociation of the MyD88-TRAM complex (Figure 2), although the mechanism underlying the dissociation and its relevance to signal regulation remain to be elucidated.

The TRAM Interaction Sites of MyD88 are Similar to that for Mal

According to our previous study [12], Sites I, II, and III on the MyD88-TIR are functionally important in TLR4 signaling. These sites also were recognized to be important in IL-18 signaling (Figure 6A and 6B). We further demonstrated that Sites II and III act as the TRAM binding sites of the MyD88 TIR domain (Figure 6C), which overlap with the Mal binding sites [12]. The two sites are distantly located from each other on opposite molecular surfaces of the protein. Because of the molecular size of the TIR domain, it is unlikely that both sites present a simultaneous binding interface for a single TRAM-TIR to form a 1:1 complex. It is more likely that each of these sites constitutes a distinct interface for a different TRAM molecule in different binding modes. Consistent with this hypothesis, a mutation of either Arg196 or Arg288 leads to only moderate losses in the binding to the TRAM-TIR in contrast to the fact that simultaneous

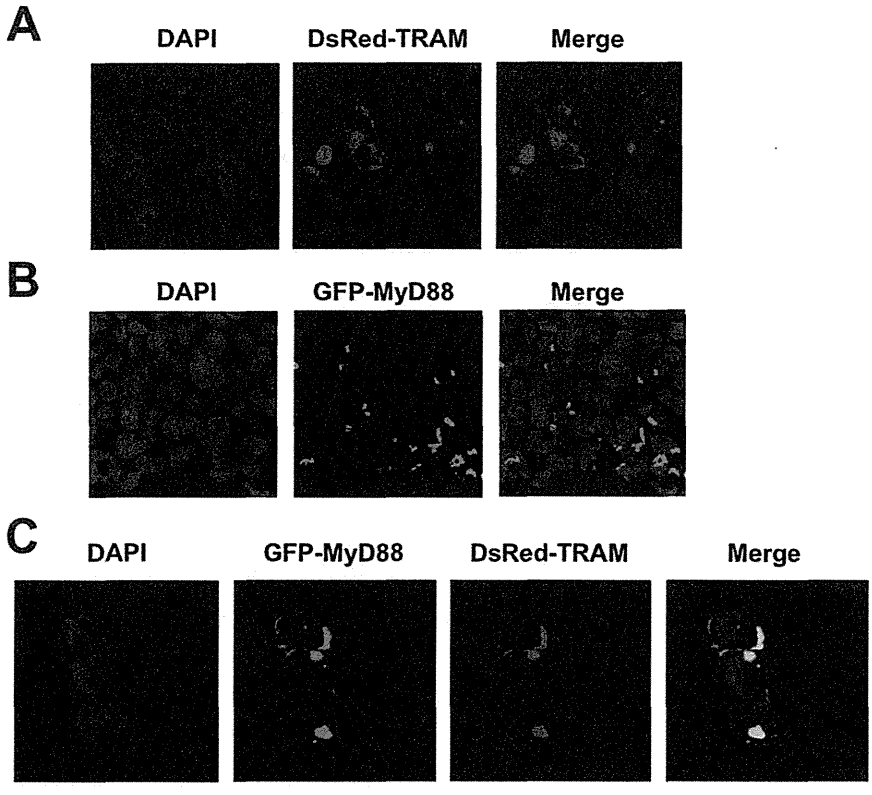

Figure 5. The localization of the MyD88 and TRAM complex in cells. (A–C) The localizations of the DsRed-TRAM (Red) and/or GFP-MyD88 (Green) in HEK293T cells. DAPI stained nuclei of HEK293T cells are shown in blue. Complexes of the DsRed fusion protein and GFP fusion protein are shown in yellow.
doi:10.1371/journal.pone.0038423.g005

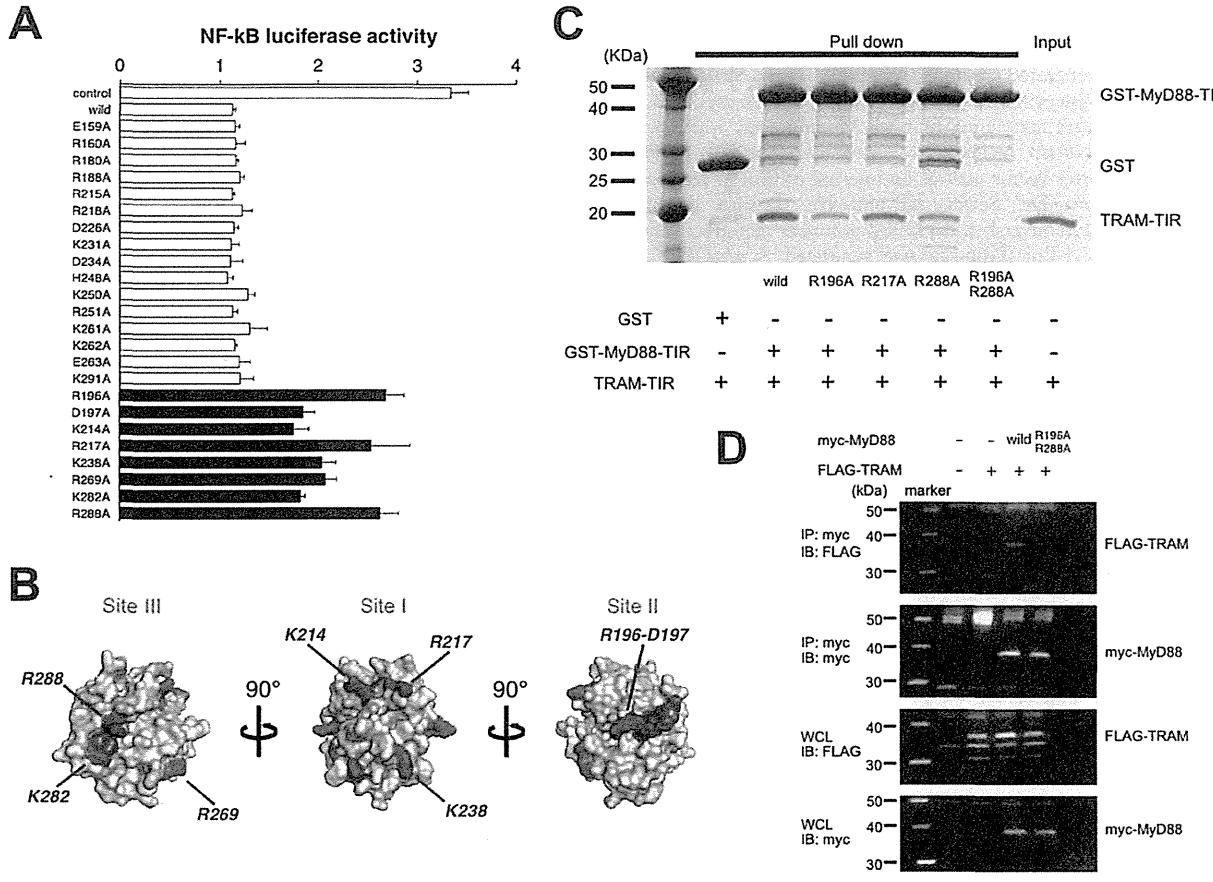

Figure 6. The interaction sites of MyD88 with TRAM. (A) Luciferase reporter gene activities with wild type and mutant types of the MyD88 TIR domain after IL-18 stimulation. The black bars indicate that the residues show significant difference with wild type. (B) The functional assays of IL-18 signaling presented on the 3D structure of the TIR domain of MyD88. Results of the functional assays are mapped onto the molecular surface of the MyD88 TIR domain. The amino acid residues judged to be significant by the luciferase assay are shown in red, while non-significant ones are shown in light brown. The conserved motifs of boxes 1–3 (FDA of box1, VLPG of box2, FW of box3) are shown in blue. (C) Assay to study the binding of the wild type or mutant TRAM TIR domain and MyD88 TIR domain. The representative alanine substitutions at Site II (R196A) or Site III (R288A) in MyD88 caused a reduced interaction with TRAM. The double alanine substituted mutant at Site II and Site III caused the complete abrogation of the interaction with TRAM. (D) Immunoprecipitation assay between MyD88 wild or R196A–R288A mutant, and TRAM.
doi:10.1371/journal.pone.0038423.g006

mutations at both residues leads to a total loss of binding (Figure 6C and 6D). With this dual binding mode via Sites II and III, TRAM would be more efficient at recruiting MyD88 to membrane regions. It should be noted that this dual binding mode was also found in the binding between the MyD88-TIR and Mal-TIR [12], which implies that this sort of multiple binding mode is common to the TIR-containing adaptor proteins.

Additionally, in human, the deficiencies of TIR domain containing adaptors, MyD88 and TRIF, have been recently reported [29,30]. These deficiencies were categorized into the innate immune defects. One of the mutations of MyD88, R196C, is known to cause the severe pyogenic bacteria infection due to the loss of interaction between TLR2, Mal and MyD88 [12]. According to the above-mentioned results, Arg196 is one of the binding sites of MyD88 to TRAM. Therefore, the substitution of Arg196 may abrogate not only an initial signaling of TLR mediated by the interaction between Mal and MyD88 but also a secondary enhancement of immune responses mediated by IL-18 induced interaction between TRAM and MyD88 in T cells or NK cells for etiology of human MyD88 deficiency syndrome.

In summary, we have established an unexpected connection between TRAM and IL-18 signaling, which is mediated by a direct TIR-TIR interaction between MyD88 and TRAM, and we proposed that TRAM is the sorting adaptor for IL-18 signaling. Based on the results obtained in this study, we present a schematic model for signal initiation from activated IL-18 (Figure S2) that is similar to the model for the LPS/TLR4 system.

Materials and Methods

Vector Preparations

The following recombinant protein expression cassettes were subcloned into pGEX4T-1, pGEX5X-1 or pGEX5X-3 (GE Healthcare, Buckinghamshire, England): IL-18, IL-1β, MyD88-TIR (amino acid residues 148–296), TRAM-TIR (66–235), TLR1-TIR (625–786), IL-18Rα-TIR (374–541), and IL-18Rβ-TIR (407–599). A cDNA encoding the MyD88 TIR domain tagged at the N-terminus with a Myc-epitope was cloned into the plasmid vector pcDNA3.1+ (Invitrogen, California, USA). IL-18Rβ and TRAM constructs tagged at the C-terminus with an

AU1- or FLAG-epitope, respectively, were also cloned into pcDNA3.1+. Mutants of TRAM and the TIR domain of MyD88 were generated using the GeneEditor *in vitro* Site-Directed Mutagenesis System (Promega, Wisconsin, USA). A pGL3-Basic Vector (Promega) containing four κB binding sites, which was used in the NF-κB luciferase reporter assay, and a Renilla luciferase reporter vector used as an internal control in the assay were gifts from Dr. Sewon Ki and Dr. Tetsuro Kokubo (Yokohama City University). An IFN-β promoter region sequence containing pGL4-Luc (Promega) was generated. A pAcGFP-C1-MyD88 (GFP-MyD88) and a pDsRed-Monomer-N1-TRAM (DsRed-TRAM) were also generated (Takara Bio, Shiga, Japan).

Protein Expression and GST Pull Down Assay

The TIR domain of the MyD88 wild type and mutants (R196A, R217A, R288A, and R196A-R288A) and the IL-18 receptors (Rα and Rβ) were purified as GST (glutathione S-transferase) fusion proteins according to methods previously described (1). The TIR domain of human TRAM and TLR1 was also obtained by a similar procedure as previously described for the MyD88-TIR. These purified proteins were incubated with Glutathione Sepharose 4B (GE Healthcare) for three hours at 4°C, and then these resins were washed four times with wash buffer (20 mM potassium phosphate buffer (pH 6.0), 100 mM KCl, 0.1 mM EDTA, 10 mM DTT, and 0.5% Triton X100), and then analyzed by SDS polyacrylamide gel electrophoresis with Coomassie Brilliant Blue staining. Experiments were performed in triplicate. The mature form of human IL-18 and IL-1β were prepared using E.Coli expression system according to previously reported methods [15].

Cell Culture

HEK293-hTLR4-MD2-CD14 cells were purchased from Invivogen (California, USA), respectively. HEK293 cells were cultured in Dulbecco's Modified Eagle Medium (high glucose-containing D-MEM, Invitrogen) supplemented with 10% heat-inactivated fetal bovine serum (SIGMA-ALDRICH, Missouri, USA), penicillin (100 U/mL) and streptomycin (100 μg/mL). All cells were incubated at 37°C in a humidified atmosphere of 5% CO2. The splenic pan T cells were isolated using Pan T Cell Isolation Kit II (Miltenyi Biotec, Bergisch Gladbach, Germany) from the spleen of TRAM-deficient mice, MyD88-deficient mice and background mice (C57BL/6) supplied by Oriental Bio Service (Kyoto, Japan). The purified splenic T cells were incubated with or without 2 ng/ml recombinant murine IL-12 (p70) (PEPROTECH, New Jersey, USA) on BIOCOAT anti-mouse CD3 T-cell activation plates (BD Biosciences, Massachusetts, USA) in order to be differentiated into Th1 cells. After 4 days of culture, T cells were washed and restimulated with 20 ng/ml recombinant murine IL-18 (MBL, Nagoya, Japan) and/or 2 ng/ml recombinant murine IL-12 (p70) on anti-mouse CD3 T-cell activation plates for 24 hours. All animal experiments were carried out in accordance with the NIH Guide for Care and Use of Laboratory Animals. These cells were cultured in RPMI1640 media (Invitrogen) supplemented with 10% heat-inactivated fetal bovine serum, penicillin (100 U/mL) and streptomycin (100 μg/mL).

Co-immunoprecipitation Analysis

HEK293T cells in 100 mm plates were transfected with 5.0 μg of pcDNA3.1+ IL-18Rβ, 5.0 μg of pcDNA3.1+ Myc-tagged MyD88 (full-length) wild or R196A-R288A mutant and/or 5.0 μg of pcDNA3.1+ FLAG-tagged TRAM (full-length) using Lipofectamine 2000 (Invitrogen). After 18 hours, the culture media were replaced. After 24 more hours, the cells were incubated with or without IL-18 (10 ng/mL). These cells were washed with cold PBS and harvested with cell lysis buffer (Tris-HCl buffer (pH 7.5) with 10 mM NaCl, 10 mM EDTA, 0.5% Triton-X100, a protease inhibitor cocktail (Roche Diagnostics, Mannheim, Germany), and a phosphatase inhibitor cocktail (PIERCE, Illinois, USA). The soluble cell lysates including 1000 μg protein were incubated with 5 μg of anti-Myc antibody (Invitrogen) or anti-FLAG M2 monoclonal antibody (SIGMA-ALDRICH) for 60 minutes; 50 μl of MultiMACS Protein G MicroBeads (Miltenyi Biotec) that had been equilibrated with cell lysis buffer for 30 minutes at 4°C was then added to the lysates. After incubation, the immune complexes were applied to the magnetic columns. The protein complex samples were then solubilized with 1× Laemmli sample buffer after four washes with wash buffer. The samples were analyzed by western blots using an anti-Myc antibody and an anti-FLAG M2 monoclonal antibody.

Knock-down with shRNA or Dominant Negative Mutant of TRAM

The shRNA expression vector psiRNA-h7SKgz-Scr (used as a negative control because it contained a scrambled sequence) and psiRNA-TICAM-2 were purchased from Invivogen. For the reporter gene assays, HEK293T or HEK293-hTLR4-MD2-CD14 cells were seeded at a density of 2.0×10^5 cells/mL per well in a 96-well plate. These cells were transfected with or without pcDNA3.1+ IL-18Rβ-AU1, NF-κB luciferase reporter vector, and Renilla luciferase reporter vector with either the psiRNA-h7SKgz-Scr or psiRNA-TICAM-2, pcDNA3.1+ TRAM-FLAG wild or C117H mutant vector using Lipofectamine 2000. After 18 hours, the culture media were replaced with fresh medium, and after an additional 24-hour incubation, the culture media were replaced with fresh medium containing recombinant human IL-18 (2.0, 5.0, 50.0 or 10.0 ng/mL) or LPSO127: B8, which is derived from *E. Coli* strain (100 ng/mL) (SIGMA-ALDRICH), incubated for 6 hours. The luciferase reporter gene activities were analyzed using a Dual-Luciferase Reporter Assay System (Promega). The statistical significance of the differences in the luciferase activities was determined using Dunnett's multiple comparison test. The statistical significance was assigned to be $P<0.05$.

RT-PCR

Total RNA from cells seeded in six-well plates was isolated with ISOGEN (Nippon Gene, Toyama, Japan) according to the manufacturer's instructions. Reverse transcription was performed with a 1st Strand cDNA Synthesis Kit (Roche Diagnostics) according to the manufacturer's instructions. The cDNA obtained was used in PCR with Taq DNA polymerase (Toyobo, Osaka, Japan) to determine the relative amount of TRAM mRNA.

ELISA

Culture supernatants in test tubes were centrifuged to remove the cells and then stored at −80°C until analysis. The IFN-γ concentrations were measured using a Mouse IFN-γ Quantikine ELISA Kit (R&D Systems, Minnesota, USA). The statistical significance of the differences in the cytokine productions between the wild type cells and the TRAM or MyD88 deficient cells was determined using two-way ANOVA with Bonferroni's multiple comparison test. The statistical significance was assigned to be $P<0.05$.

Confocal Microscopy

For direct immunofluorescence, HEK293T cells co-transfected GFP-MyD88 and DsRed-TRAM were washed in phosphate-

buffered saline and fixed for 10 min in 4% paraformaldehyde in phosphate-buffered saline. Cells were then permeabilized with 0.2% Triton X-100 in phosphate buffered saline for 10 min at room temperature. Samples were mounted onto coverslips with Pro-Long Gold Antifade reagent (Invitrogen) and were examined on a Zeiss LSM5 EXCITER confocal microscope. All images were acquired using an aplan-Apochrom at 63X with a 1.4-N.A. objective or at 100X with a 1.4-N.A. objective.

The Screening Method of Functional Residues of MyD88-TIR in IL-18 Signaling

HEK293T cells were transfected with pcDNA3.1+ control vector or pcDNA3.1+ myc-MyD88 TIR domain (wild-type or mutants), pcDNA3.1+ IL-18Rβ-AU1, NF-κB luciferase reporter vector, and Renilla luciferase reporter vector using Lipofectamine 2000 according to the manufacturer's instructions. These transfectants were stimulated with recombinant human IL-18 (100 ng/mL) for 6 hours. The luciferase reporter gene activities were also analyzed using a Dual-Luciferase Reporter Assay System (Promega). The statistical significance of the differences was determined using Dunnett's multiple comparison test. The statistical significance was assigned to be $P<0.05$.

Supporting Information

Figure S1 The surface electrostatic potential of the TIR domain structure models from the TIR domain containing adaptor proteins. These structure models were predicted from the template structure of the MyD88-TIR (PDB code: 2z5v) using Discovery Studio 2.6 software (Accelrys). TRAM and MAL have a largely acidic surface patch, while MyD88 has a largely basic surface patch.
(TIFF)

Figure S2 A schematic model of the two distinct regulation patterns in LPS induced TLR4 signaling and IL-18 signaling. MyD88 is efficiently delivered to receptor specific membrane regions by the membrane binding activities of the two associated molecules of Mal or TRAM so that it can form signal initiation complexes with activated TLR4 or IL-18 receptors. Upon stimulation, MyD88 starts to transmit signals through interactions with activated TLR4 or IL-18R, which triggers the phosphorylation cascade mediated by IRAKs and TRAF6.
(TIFF)

Acknowledgments

We thank Dr. T. Fukao, Dr. H. Kaneko, Dr. K Hirayama, and K. Kasahara for their advice and technical help. We thank Dr. S. Ki and Dr. T. Kokubo for their kind gift of vector samples.

Author Contributions

Conceived and designed the experiments: HO HT ZK MS N. Kondo. Performed the experiments: HO HT N. Kawamoto TK KK TY TF HN RW. Analyzed the data: HO HT RW MS. Wrote the paper: HO HT ZK RW MS.

References

1. Akira S, Uematsu S, Takeuchi O (2006) Pathogen recognition and innate immunity. Cell 124: 783–801.
2. Kawai T, Akira S (2007) Signaling to NF-kappaB by Toll-like receptors. Trends Mol Med 13: 460–469.
3. Bonnert TP, Garka KE, Parnet P, Sonoda G, Testa JR, et al. (1997) The cloning and characterization of human MyD88: a member of an IL-1 receptor related family. FEBS Lett 402: 81–84.
4. Lin SC, Lo YC, Wu H (2010) Helical assembly in the MyD88-IRAK4-IRAK2 complex in TLR/IL-1R signalling. Nature 465: 885–890.
5. Kagan JC, Medzhitov R (2006) Phosphoinositide-mediated adaptor recruitment controls Toll-like receptor signaling. Cell 125: 943–955.
6. Yamamoto M, Sato S, Hemmi H, Sanjo H, Uematsu S, et al. (2002) Essential role for TIRAP in activation of the signalling cascade shared by TLR2 and TLR4. Nature 420: 324–329.
7. Kenny EF, Talbot S, Gong M, Golenbock DT, Bryant CE, et al. (2009) MyD88 adaptor-like is not essential for TLR2 signaling and inhibits signaling by TLR3. J Immunol 183: 3642–3651.
8. Kagan JC, Su T, Horng T, Chow A, Akira S, et al. (2008) TRAM couples endocytosis of Toll-like receptor 4 to the induction of interferon-beta. Nat Immunol 9: 361–368.
9. Tanimura N, Saitoh S, Matsumoto F, Akashi-Takamura S, Miyake K (2008) Roles for LPS-dependent interaction and relocation of TLR4 and TRAM in TRIF-signaling. Biochem Biophys Res Commun 368: 94–99.
10. Rowe DC, McGettrick AF, Latz E, Monks BG, Gay NJ, et al. (2006) The myristoylation of TRIF-related adaptor molecule is essential for Toll-like receptor 4 signal transduction. Proc Natl Acad Sci U S A 103: 6299–6304.
11. Horng T, Barton GM, Flavell RA, Medzhitov R (2002) The adaptor molecule TIRAP provides signalling specificity for Toll-like receptors. Nature 420: 329–333.
12. Ohnishi H, Tochio H, Kato Z, Orii KE, Li A, et al. (2009) Structural basis for the multiple interactions of the MyD88 TIR domain in TLR4 signaling. Proc Natl Acad Sci U S A 106: 10260–10265.
13. O'Neill LA, Bowie AG (2007) The family of five: TIR-domain-containing adaptors in Toll-like receptor signalling. Nat Rev Immunol 7: 353–364.
14. Brown V, Brown RA, Ozinsky A, Hesselberth JR, Fields S (2006) Binding specificity of Toll-like receptor cytoplasmic domains. Eur J Immunol 36: 742–753.
15. Kato Z, Jee J, Shikano H, Mishima M, Ohki I, et al. (2003) The structure and binding mode of interleukin-18. Nat Struct Biol 10: 966–971.
16. Fitzgerald KA, Rowe DC, Barnes BJ, Caffrey DR, Visintin A, et al. (2003) LPS-TLR4 signaling to IRF-3/7 and NF-kappaB involves the toll adapters TRAM and TRIF. J Exp Med 198: 1043–1055.
17. Nishiya T, Kajita E, Horinouchi T, Nishimoto A, Miwa S (2007) Distinct roles of TIR and non-TIR regions in the subcellular localization and signaling properties of MyD88. FEBS Lett 581: 3223–3229.
18. Yamamoto M, Sato S, Hemmi H, Uematsu S, Hoshino K, et al. (2003) TRAM is specifically involved in the Toll-like receptor 4-mediated MyD88-independent signaling pathway. Nat Immunol 4: 1144–1150.
19. Bin LH, Xu LG, Shu HB (2003) TIRP, a novel Toll/interleukin-1 receptor (TIR) domain-containing adapter protein involved in TIR signaling. J Biol Chem 278: 24526–24532.
20. Oshiumi H, Sasai M, Shida K, Fujita T, Matsumoto M, et al. (2003) TIR-containing adapter molecule (TICAM)-2, a bridging adapter recruiting to toll-like receptor 4 TICAM-1 that induces interferon-beta. J Biol Chem 278: 49751–49762.
21. Dunne A, Ejdeback M, Ludidi PL, O'Neill LA, Gay NJ (2003) Structural complementarity of Toll/interleukin-1 receptor domains in Toll-like receptors and the adaptors Mal and MyD88. J Biol Chem 278: 41443–41451.
22. Sheedy FJ, O'Neill LA (2007) The Troll in Toll: Mal and Tram as bridges for TLR2 and TLR4 signaling. J Leukoc Biol 82: 196–203.
23. Sacre SM, Lundberg AM, Andreakos E, Taylor C, Feldmann M, et al. (2007) Selective use of TRAM in lipopolysaccharide (LPS) and lipoteichoic acid (LTA) induced NF-kappaB activation and cytokine production in primary human cells: TRAM is an adaptor for LPS and LTA signaling. J Immunol 178: 2148–2154.
24. Choi YJ, Im E, Chung HK, Pothoulakis C, Rhee SH (2010) TRIF mediates Toll-like receptor 5-induced signaling in intestinal epithelial cells. J Biol Chem 285: 37570–37578.
25. Medvedev AE, Piao W, Shoenfelt J, Rhee SH, Chen H, et al. (2007) Role of TLR4 tyrosine phosphorylation in signal transduction and endotoxin tolerance. J Biol Chem 282: 16042–16053.
26. Piao W, Song C, Chen H, Wahl LM, Fitzgerald KA, et al. (2008) Tyrosine Phosphorylation of MyD88 Adapter-like (Mal) Is Critical for Signal Transduction and Blocked in Endotoxin Tolerance. J Biol Chem 283: 3109–3119.
27. McGettrick AF, Brint EK, Palsson-McDermott EM, Rowe DC, Golenbock DT, et al. (2006) Trif-related adapter molecule is phosphorylated by PKC{epsilon} during Toll-like receptor 4 signaling. Proc Natl Acad Sci U S A 103: 9196–9201.
28. Seykora JT, Myat MM, Allen LA, Ravetch JV, Aderem A (1996) Molecular determinants of the myristoyl-electrostatic switch of MARCKS. J Biol Chem 271: 18797–18802.
29. Sancho-Shimizu V, Perez de Diego R, Lorenzo L, Halwani R, Alangari A, et al. (2011) Herpes simplex encephalitis in children with autosomal recessive and dominant TRIF deficiency. The Journal of clinical investigation 121: 4889–4902.
30. von Bernuth H, Picard C, Jin Z, Pankla R, Xiao H, et al. (2008) Pyogenic bacterial infections in humans with MyD88 deficiency. Science 321: 691–696.

Molecular Immunology 52 (2012) 108–116

Contents lists available at SciVerse ScienceDirect

Molecular Immunology

journal homepage: www.elsevier.com/locate/molimm

Molecular analysis of the binding mode of Toll/interleukin-1 receptor (TIR) domain proteins during TLR2 signaling

Masatoshi Nada[a,b], Hidenori Ohnishi[a,*], Hidehito Tochio[c], Zenichiro Kato[a], Takeshi Kimura[a,d], Kazuo Kubota[a], Takahiro Yamamoto[a], Yuji O. Kamatari[e], Naotaka Tsutsumi[c], Masahiro Shirakawa[c,f], Naomi Kondo[a]

[a] Department of Pediatrics, Graduate School of Medicine, Gifu University, Yanagido 1-1, Gifu 501-1194, Japan
[b] Kumiai Welfare Hospital, Ohshinmachi 5-68, Takayama, Gifu 506-8502, Japan
[c] Department of Molecular Engineering, Graduate School of Engineering, Kyoto University, Katsura, Nishikyo-ku, Kyoto 615-8510, Japan
[d] Neonatal Intensive Care Unit, Department of Pediatrics, Graduate School of Medicine, Gifu University, Yanagido 1-1, Gifu 501-1194, Japan
[e] Life Science Research Center, Gifu University, Yanagido 1-1, Gifu 501-1194, Japan
[f] Core Research for Evolutional Science and Technology, Japan Science and Technology Corporation, Hon-cho 4-1-8, Kawaguchi, Saitama 332-0012, Japan

ARTICLE INFO

Article history:
Received 23 September 2011
Received in revised form 23 April 2012
Accepted 1 May 2012
Available online 4 June 2012

Keywords:
Innate immunity
MyD88
Mal
TIRAP
TIR domain
TLR2

ABSTRACT

Toll-like receptor (TLR) signaling is initiated by the binding of various adaptor proteins through ligand-induced oligomerization of the Toll/interleukin-1 receptor (TIR) domains of the TLRs. TLR2, which recognizes peptidoglycans, lipoproteins or lipopeptides derived from Gram-positive bacteria, is known to use the TIR domain-containing adaptor proteins myeloid differentiating factor 88 (MyD88) and MyD88 adaptor-like (Mal). Molecular analyses of the binding specificity of MyD88, Mal, and TLR2 are important for understanding the initial defenses mounted against Gram-positive bacterial infections such as *Streptococcus pneumoniae*. However, the detailed molecular mechanisms involved in the multiple interactions of these TIR domains remain unclear. Our study demonstrates that the TIR domain proteins MyD88, Mal, TLR1, and TLR2 directly bind to each other *in vitro*. We have also identified two binding interfaces of the MyD88 TIR domain for the TLR2 TIR domain. A residue at these interfaces has recently been found to be mutated in innate immune deficiency patients. These novel insights into the binding mode of TIR proteins will contribute to elucidation of the mechanisms underlying innate immune deficiency diseases, and to future structural studies of hetero-oligomeric TIR–TIR complexes.

1. Introduction

The innate immune system is the first line of host defense against pathogens. Toll-like receptors (TLRs) are known to be essential sensors of infectious microorganisms by the immune system. TLRs can recognize common molecular structures detected in certain groups of microorganisms, which are described as pathogen-associated molecular patterns (PAMPs) (Akira et al., 2006). PAMPs include bacterial cell wall components such as lipopolysaccharide (LPS), which is contained in the cell walls of Gram-negative bacteria and is recognized by TLR4. Gram-positive bacteria do not carry LPS, but their cell walls contain a thick layer of peptidoglycans and a number of lipoproteins or lipopeptides. These components are recognized by TLR2 and TLR1 or TLR10 (Guan et al., 2010). Intracellularly, TLR signaling is initiated by the binding of various adaptor proteins to the Toll/interleukin-1 receptor (TIR) domains of activated TLRs. Five adaptors containing the TIR domain have been identified: myeloid differentiating factor 88 (MyD88); MyD88 adaptor-like (Mal); TIR domain-containing adaptor-including IFN-β (TRIF); TRIF-related adaptor molecule (TRAM); and sterile α and huntingtin-elongation-A subunit-TOR Armadillo motifs (SARM) (O'Neill and Bowie, 2007). Recruitment of one or more of these adaptors to a TLR initiates signaling events that activate transcription factors such as NF-κB, activator protein 1 (AP-1), and/or interferon regulatory factor (IRF) families (Kawai and Akira, 2007).

Abbreviations: PAMPs, pathogen-associated molecular patterns; MyD88, myeloid differentiating factor 88; Mal, MyD88 adaptor-like; TIR, Toll/interleukin-1 receptor; TRIF, TIR domain-containing adaptor-including IFN-β; TRAM, TRIF-related adaptor molecule; SARM, sterile α and huntingtin-elongation-A subunit-TOR Armadillo motifs; AP-1, activator protein 1; IRF, interferon regulatory factor; PIP2, phosphatidylinositol 4,5-bisphosphate; IRAK-4, IL-1 receptor-associated kinase-4; NEMO, NF-κB essential modulator; MyD88-TIR, TIR domain of MyD88; Mal-TIR, TIR domain of Mal; TLR1-TIR, TIR domain of TLR1; TLR2-TIR, TIR domain of TLR2; TLR4-TIR, TIR domain of TLR4; Pam3CSK4, $Pam_3Cys\text{-}Ser\text{-}(Lys)_4$; HSQC, hetero-nuclear single quantum coherence; HEK, human embryonic kidney.

* Corresponding author. Tel.: +81 58 230 6386; fax: +81 58 230 6387.
E-mail address: ohnishih@gifu-u.ac.jp (H. Ohnishi).

0161-5890/$ – see front matter © 2012 Elsevier Ltd. All rights reserved.
http://dx.doi.org/10.1016/j.molimm.2012.05.003

In innate immune responses, MyD88 has pivotal functions in the formation of signal initiation complexes involving the cytosolic domain of TLRs. MyD88 has been reported to be involved in the signaling pathways initiated by all TLRs thus far reported, with the exception of TLR3 (Kaisho and Akira, 2006). Of the MyD88-dependent pathways involving TLR2, -4, -5, -7, and -9, only the TLR2 (including TLR1, TLR6 and TLR10) and TLR4 pathways require Mal for efficient signal transduction (Horng et al., 2002). Recently, Kagan and Medzhitov (2006) revealed that MyD88 and Mal have distinctly different roles in TLR4 signaling: MyD88 serves as an essential "signaling adaptor", which transmits signals from ligand-activated TLRs to downstream factors to initiate kinase-dependent signaling cascades, while Mal functions as a "sorting adaptor", which recruits MyD88 to the plasma membrane *via* its phosphatidylinositol 4,5-bisphosphate (PIP2) binding domain to promote interaction between MyD88 and activated TLR4 beneath the membrane. Indeed, one of our previous studies also suggested that Mal mediates TIR–TIR interactions between TLR4 and MyD88 (Ohnishi et al., 2009).

Thus, while the clear role divisions between MyD88 and Mal in TLR4 signaling have been demonstrated, only limited information is available about their roles in TLR2 signaling. The MAPPIT (Mammalian Protein–Protein Interaction Trap) system showed that Mal was able to enhance both TLR2 and TLR4 signaling (Ulrichts et al., 2007). This finding suggests that Mal is necessary for TLR2 signaling and for the formation of a TLR2/Mal/MyD88 bridging complex. In contrast, other reports have shown that Mal is dispensable for TLR2 signaling at high concentrations of the TLR1/2 ligand, and is only essential at low ligand concentrations (Kenny et al., 2009; Santos-Sierra et al., 2009). Therefore, it has been suggested that Mal acts to enhance TLR2 signaling, but is not essential for transduction of the signal.

Recently, human primary immunodeficiency diseases in innate immunity such as MyD88 and IL-1 receptor-associated kinase-4 (IRAK-4) deficiencies, and ectodermal dysplasia with immunodeficiency have been reported (Picard et al., 2011). In addition, several polymorphisms in TLRs have been reported as being associated with immune disorders (Arbour et al., 2000; Khor et al., 2007). Patients with MyD88 deficiency and IRAK-4 deficiency have been found to be highly susceptible to Gram-positive bacteria, while showing normal resistance to most other kinds of pathogens, such as viruses, widespread bacteria, parasites, and fungi. These phenotypes suggest that TLR2 signaling, which is initiated by peptidoglycan and lipoprotein in Gram-positive bacteria, is more dependent on MyD88/IRAK-4 signaling than other self-defense systems in early life, possibly owing to redundancy in other innate immune signaling pathways. To understand the mechanisms of MyD88 and IRAK-4 deficiencies, it is necessary to analyze the intricacies of the interactions between MyD88 and other signaling components.

Hetero-oligomeric interactions between TIR domains from receptor and adaptor proteins play pivotal roles in these signal transduction systems, as do the hetero-oligomeric interactions of death domain family proteins, but only limited structural information about such interactions is available. Several isolated protein structures of TIR domains have recently been reported (Nyman et al., 2008; Ohnishi et al., 2009; Valkov et al., 2011; Xu et al., 2000); however, the detailed interaction mode of the TIR–TIR domains remains unclear.

Our present study investigated direct interactions between TIR domains involved in TLR2 signaling. *In vitro* binding experiments using purified proteins demonstrated that the TIR domain of MyD88 (MyD88-TIR) directly bound to the cytosolic TIR domain of TLR1, TLR2, and Mal. In addition, we identified four functional residues of the MyD88-TIR that are important for the Pam_3Cys-Ser-$(Lys)_4$ (Pam3CSK4)-activated TLR1/2 signaling pathway, as well as for the LPS-activated TLR4 signaling pathway. Furthermore, we identified two binding interfaces of MyD88-TIR for the TIR domain of TLR2 (TLR2-TIR), both of which are shared with Mal. One of these interfaces includes a residue for which a missense mutation causes pyogenic bacterial infections. These analyses of the detailed molecular interaction mechanisms will contribute to elucidation of the etiology underlying recently identified innate immune deficiency diseases and lead to further structural studies.

2. Materials and methods

2.1. Protein sample preparation

The TIR domains of human TLR1, TLR2, MyD88 and Mal were purified using the following modification to previously reported methods (Ohnishi et al., 2009; Tao and Tong, 2009). The portions of the human TLR1 gene encoding the TIR domain (amino acid residues 625–786), the TLR2 gene encoding the TIR domain (amino acid residues 633–784), the MyD88 gene encoding the TIR domain (amino acid residues 148–296), and the Mal gene encoding the TIR domain (amino acid residues 75–235), were each cloned separately into a pGEX-5X-3 vector (GE Healthcare, Buckinghamshire, England). The constructs were transformed into *Escherichia coli* BL-21 (DE3) (Novagen, Darmstadt, Germany). The TIR domains, expressed as GST fusion proteins, were initially purified by glutathione Sepharose 4B FF (GE Healthcare) affinity chromatography, and the GST-tag was removed by digestion with Factor Xa (GE Healthcare). Subsequently, the TIR domains were purified by gel filtration (Sephacryl S-200 HR 16/60 column; GE Healthcare, Buckinghamshire, England). ^{15}N-labeled TIR domain proteins were prepared using the same purification protocol. All NMR samples were uniformly ^{15}N-labeled and prepared in 250 μl solutions of H_2O/D_2O (90%/10%) containing 20 mM potassium phosphate buffer at pH 6.0, 10 mM DTT and 0.1 mM EDTA. The ^{15}N-labeled protein concentration was approximately 0.02 mM for all of the NMR samples.

2.2. NMR spectroscopy

Two-dimensional (2D) ^1H–^{15}N correlation spectrum for the TIR domains of TLR1 was measured using a hetero-nuclear single quantum coherence (HSQC) pulse sequence on a Varian Innova 900 MHz spectrometer. The 2D ^1H–^{15}N correlation spectrum for the TIR domains of TLR2 was measured using a HSQC pulse sequence on a Bruker Avance 800 MHz spectrometer equipped with a cryogenic probe. The 2D ^1H–^{15}N correlation spectra of the TIR domains of MyD88 (wild-type and mutants) and Mal were measured on a Bruker Avance II 700 MHz spectrometer equipped with a cryogenic probe using a HSQC and a SOFAST-HMQC pulse sequence (Schanda and Brutscher, 2005), respectively. All spectra were recorded at 25 °C. For the HSQC spectrum of the TIR domain of TLR1, the matrix size acquired was 100 (t1) and 1864 (t2) complex points with spectral widths of 2553.72 Hz (F1) and 14,383.32 Hz (F2). For the HSQC spectrum of the TIR domain of TLR2, the matrix size acquired was 128 (t1) and 1024 (t2) complex points with spectral widths of 2432.73 Hz (F1) and 12,019.23 Hz (F2). For the HSQC spectra of the wild-type and mutant TIR domains of MyD88, the matrix size acquired was 64 (t1) and 1024 (t2) complex points with spectral widths of 2128.46 Hz (F1) and 11,261.26 Hz (F2). For the SOFAST-HMQC spectrum of the TIR domain of Mal, the matrix size acquired was 64 (t1) and 256 (t2) complex points with spectral widths of 2483.54 Hz (F1) and 5597.01 Hz (F2). The acquired FID data were apodized with a squared cosine-bell window function and zero-filled to double the data points in both dimensions prior to Fourier transformation. All NMR spectra were processed and analyzed with

NMRPipe (Delaglio et al., 1995) and Sparky (Goddard and Kneller, 1999) software.

2.3. Cell culture

Human embryonic kidney (HEK) 293-hTLR1/2 cells were purchased from InvivoGen (San Diego, CA). Cells were cultured in Dulbecco's modified Eagle's medium (high glucose-containing; InvivoGen) supplemented with 10% heat-inactivated fetal bovine serum (Sigma, St. Louis, MO), penicillin (100 U/ml), and streptomycin (100 μg/ml). Cells were incubated at 37 °C in a humidified atmosphere of 5% CO_2.

2.4. Vector preparations

A cDNA encoding the TIR domain of MyD88 (amino acid residues 148–296) or the full-length MyD88 (amino acid residues 1–296), tagged at the N terminus with a myc-epitope, was cloned into the plasmid vector pcDNA3.1+ (Invitrogen, Carlsbad, CA). Similarly, a cDNA encoding Mal (amino acid residues 1–235) was cloned into the plasmid vector pFLAG-CMV6a (Sigma). MyD88-TIR mutants of 37 charged polar amino acid residues (Asp, Glu, Arg, Lys, and His) and full-length MyD88 mutants of Arg-196, Arg-217, Lys-282, and Arg-288 substituted by alanine or cysteine were generated using the GeneEditor *in vitro* Site-Directed Mutagenesis System (Promega, Madison, WI). The vector pGL4.32[luc2P/NF-κB-RE/Hygro], which was used as an NF-κB luciferase reporter vector, and the vector pGL4.70[hRluc], which was used as a Renilla luciferase reporter vector for an internal control, were purchased from Promega.

2.5. Western blot analysis

Cells were harvested, washed with PBS, then lysed. The lysates were cleared by centrifugation at 15,000 × *g* for 5 min at 4 °C. All extracts were adjusted to contain equal amounts of total cellular proteins, as determined using the Lowry method. The supernatants were separated by electrophoresis on SDS polyacrylamide gels and transferred to nitrocellulose membranes using an iBlot Gel Transfer Device (Invitrogen, Carlsbad, CA). Membranes were blocked for 1 h in 5% BSA in TBST (10 mM Tris–HCl, pH 8.0, 0.15 M NaCl and 0.1% Tween 20), then incubated at room temperature for 2 h with an anti-myc antibody (Invitrogen), anti-FLAG antibody (Sigma), or anti-TLR2 antibody (Santa Cruz Biotechnology, Santa Cruz, CA), followed by incubation with anti-mouse or anti-rabbit IgG HRP conjugate (Promega) at room temperature for 30 min. Detection was performed using ECL-plus (Amersham, Piscataway, NJ) and lightcapture system AE6970CP (ATTO, Tokyo, Japan).

2.6. Expression of MyD88 TIR domain mutants

HEK293 cells cultured in six-well plates were transfected with 1.0 μg pcDNA3.1+ empty vector (mock) or 1.0 μg pcDNA3.1+ myc-tagged MyD88-TIR (wild type or mutants), using Lipofectamine 2000 (Invitrogen, Carlsbad, CA) according to the manufacturer's instructions. After 24 and 48 h, culture media were replaced with fresh media. The cells were then harvested using CytoBuster Protein Extraction Reagent (Novagen). The cell extracts (containing equal quantities of protein) were checked by western blot analysis using an anti-myc antibody (Invitrogen). Mutants with poor expression profiles were not included in subsequent studies to avoid potential misinterpretation of the results (*e.g.* loss of dominant negative inhibitory effect).

2.7. NF-κB reporter gene activity

293-hTLR1/2 cells were transfected with the pcDNA3.1+ empty vector (mock) or MyD88-TIR (wild-type or mutants), NF-κB luciferase reporter vector, and Renilla luciferase reporter vector, using Lipofectamine 2000. After the transfection, the cells were stimulated with synthetic tripalmitoyl lipopeptide Pam3CSK4 (0.1 μg/ml, InvivoGen), then incubated for 6 h. HEK293T cells were also transfected with the mock or full-length MyD88 (wild-type or mutants) and luciferase reporter vectors using Lipofectamine 2000, and incubated for 24 h. Luciferase reporter gene activity was analyzed using a Dual-Luciferase Reporter Assay System (Promega). The inhibitory effect of each TIR expression mutant was assessed by at least three independent experiments. The statistical significance of the differences observed in the luciferase activities between the wild-type and the mutants in the NF-κB reporter assays was determined using Dunnett's multiple comparison test. Statistical significance was assumed at P-values < 0.05.

2.8. GST pull-down assays

The TIR domains of the MyD88 wild-type and its mutants (R196C, R217A, K282A-R288A) were purified as GST-fusion proteins. These expression vectors were generated by sub-cloning the pcDNA3.1+ myc-tagged MyD88-TIR into pGEX-5X-1 (GE Healthcare, Buckinghamshire, England). GST fusion proteins were purified by glutathione Sepharose 4B FF affinity chromatography, and subsequently purified with dialysis membrane to exclude less than 30 kDa. GST-fusion proteins of the MyD88-TIR, Mal-TIR or TLR2-TIR, and purified proteins of the TIR domain of TLR1, TLR2, or Mal were incubated with Glutathione Sepharose 4B (GE Healthcare) in binding buffers (20 mM potassium phosphate buffer (pH 6.0), 0.1 mM EDTA, 10 mM DTT, 0.2% BSA and 0.5% NP-40, or 20 mM potassium phosphate buffer (pH 6.0), 10 mM DTT, and 0.5% NP-40) overnight. After four wash steps using 20 mM potassium phosphate buffer (pH 6.0), 100 mM KCl, 0.1 mM EDTA, 10 mM DTT, and 0.5% NP-40, the resin was analyzed by SDS polyacrylamide gel electrophoresis and Coomassie Brilliant Blue staining.

2.9. Immunoprecipitation assays

293-hTLR1/2 cells were co-transfected with the pcDNA3.1+ myc-tagged MyD88 and pFLAG-CMV6a Mal using Lipofectamine 2000. After transfection, the cells were stimulated with Pam3CSK4 (0.1 μg/ml, InvivoGen). The cells were then lysed using 10 mM Tris–HCl, pH 7.5, 20 mM NaCl, 10 mM EDTA and 0.5% Triton-X100, in the presence of a protease inhibitor mix (Roche Applied Science, Indianapolis, IN). The cell lysates were prepared as indicated above (2.5 Western blot analysis). The solutions containing equal quantities of protein were pretreated with the anti-TLR2 antibody (Santa Cruz Biotechnology, Santa Cruz, CA) for 1 h, and then treated with μMACS ProteinG MicroBeads (Miltenyi Biotec, Bergisch Gladbach, Germany) for 30 min at 4 °C. Subsequently, the protein concentrations were loaded onto μ Columns (Miltenyi Biotec). After washing with the lysis buffer containing protease inhibitors, the proteins were eluted with SDS-loading buffer and analyzed by western blot analysis.

3. Results

3.1. NMR analyses of TIR domains and GST pull-downs

Recombinant proteins representing the TIR domain of TLR1, TLR2, Mal, and MyD88 were expressed using an *E. coli* expression system. The 2D ^{1}H–^{15}N correlation spectra of these TIR domains

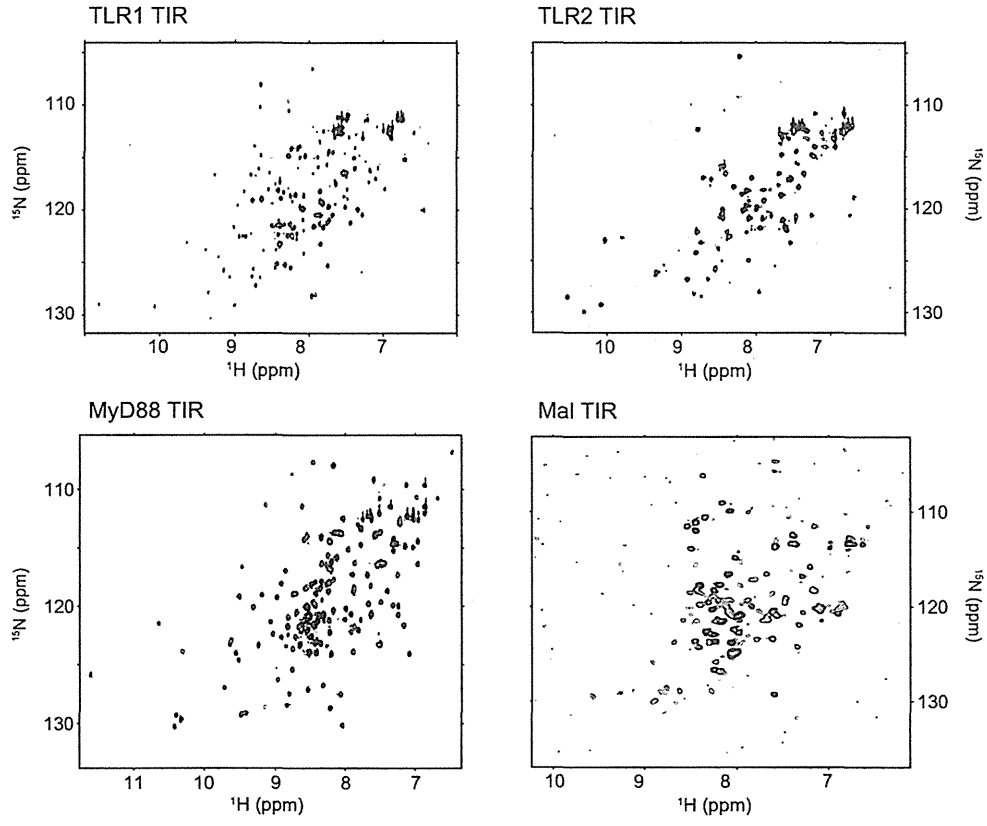

Fig. 1. ^{1}H–^{15}N correlation NMR spectra of TLR1-TIR, TLR2-TIR, MyD88-TIR and Mal-TIR. The spectra show the widespread patterns of the backbone amide ^{1}H–^{15}N cross-peaks, suggesting that the protein samples had adopted the correct folding of the TIR domains.

showed widespread patterns of the backbone amide ^{1}H–^{15}N cross-peaks (Fig. 1), suggesting that the protein samples had adopted the correct folding pattern of the TIR domain. Using GST pull-down assays, we next evaluated direct interactions between the TIR-domain proteins involved in TLR2 signaling. For these experiments, we constructed GST TIR fusion proteins for MyD88, Mal and TLR2. These proteins included no degradation and contaminant bands near the masses of the TIR domains (see Fig. S1). Our previous study showed that the TIR domain of Mal (Mal-TIR) directly binds to the TLR4-TIR, while an interaction between the TLR4-TIR and MyD88-TIR was not detected (Ohnishi et al., 2009). In the present study, TLR1-TIR, TLR2-TIR and Mal-TIR were pulled down with the GST-MyD88-TIR (Fig. 2A). Moreover, the TLR1-TIR and Mal-TIR were pulled down with GST-TLR2-TIR (Fig. 2B), while TLR1-TIR and TLR2-TIR were pulled down with GST-Mal-TIR (Fig. 2C). Hence, these results show that the TIR domain of MyD88, Mal, TLR1, and TLR2 are able to directly bind to each other.

3.2. Functional residues of the MyD88 TIR domain for TLR1/TLR2 signaling

To assess which residues are important for the function of MyD88-TIR, we performed mutational analysis of the domain, using the dominant-negative effects of ectopically expressed isolated TIR domains as a previously reported method for TLR4 signaling (Ohnishi et al., 2009). The expression levels of the MyD88-TIR alanine substitution mutants in HEK293 cells are shown in Fig. 3A. We created 37 alanine substitutions with charged amino acids of the MyD88-TIR. The expression levels of D162A, D171A, E177A, E183A, K190A, D195A, E210A, E213A, D225A, K256A, K258A and D275A were significantly lower than those of the other mutants. Analysis of the NMR solution structure of the MyD88-TIR showed that the average ratio of the molecular surface exposure of the residues (20.6 ± 12.6%), of which alanine substitutions were insufficiently expressed, was also significantly lower than that of the other residues (36.8 ± 13.5%). The differences in the ratio of molecular surface exposure were tested with an unpaired *t*-test; statistical significance was assumed to be $P < 0.05$. The results of the Pam3CSK4 stimulated NF-κB luciferase reporter gene activity assay, using 25 dominant-negative MyD88 mutants in which expression was confirmed are shown in Fig. 3B. Alanine substitutions of four residues, *i.e.* Arg-196, Arg-217, Lys-282, and Arg-288, resulted in a significantly reduced inhibitory effect in the Pam3CSK4-induced luciferase activity. Interestingly, these four residues are similar to those involved in TLR4 signaling and closely associated with the box 1, 2, and 3 motifs, which are highly conserved across TIR domains. Arg-196 is located within the box 2 motif. The side chains of Lys-282 and Arg-288 form a continuous protein surface with box 3 forming residues, and Arg-217 is located distant in the sequence, but proximal in space to the box 1 motif. Hence, we recently designated the sites that these residues form as Site II (Arg-196), Site III (Lys-282 and Arg-288), and Site I (Arg-217) (Ohnishi et al., 2009).

3.3. Two interfaces of the MyD88 TIR domain interact with the TLR2 TIR domain

Because Site I, Site II, and Site III of MyD88-TIR are important for TLR2-mediated cellular responses following Pam3CSK4 stimulation, we next examined the involvement of these sites in direct binding to TLR2-TIR. We expressed GST fusion proteins of the MyD88-TIR mutants (R196C, R217A, and K282A/R288A) using

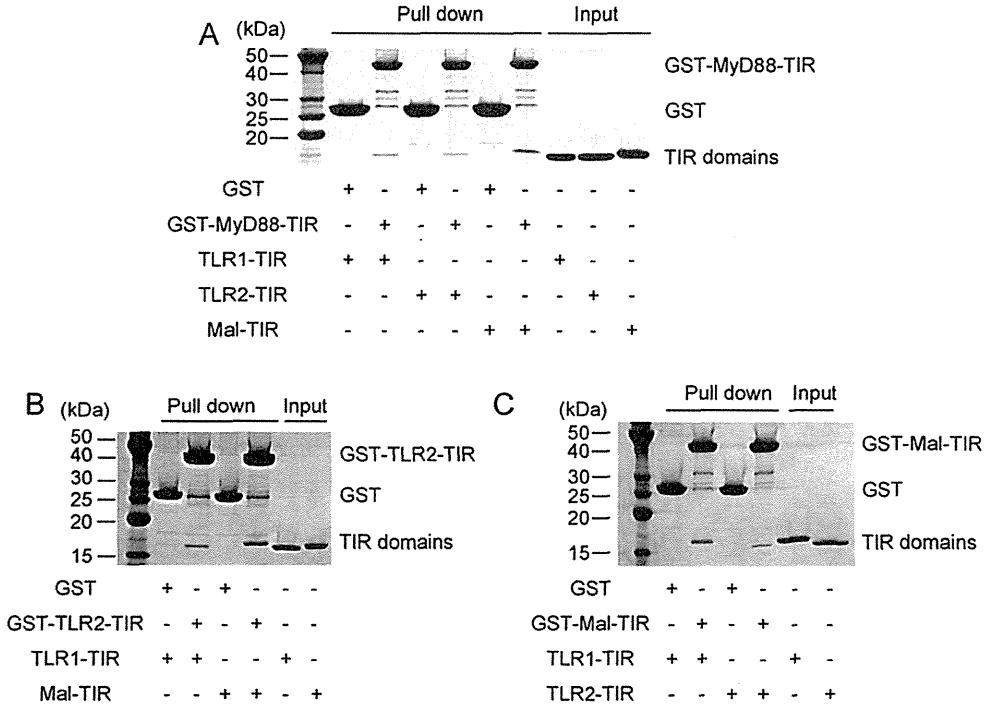

Fig. 2. Analysis of direct interactions between the TIR domains involved in TLR2 signaling using GST pull-down assays. (A) Binding assays for MyD88-TIR with TLR1-TIR, TLR2-TIR or Mal-TIR. GST-MyD88-TIR binds TLR1-TIR, TLR2-TIR and Mal-TIR. (B) Binding assay for TLR2-TIR with TLR1-TIR or Mal-TIR. GST-TLR2-TIR binds both TLR1-TIR and Mal-TIR. (C) Binding assay for Mal-TIR with TLR1-TIR or TLR2-TIR. GST-Mal-TIR binds both TLR1-TIR and TLR2-TIR.

an *E. coli* expression system (Materials and Methods). The 2D ^{1}H–^{15}N correlation spectra of the MyD88-TIR mutants showed widespread patterns in the backbone amide ^{1}H–^{15}N cross-peaks, which were mostly superimposable with that of the wild-type MyD88-TIR (Fig. 4A), indicating no substantial structural change was induced by the amino acid substitution. In the spectra of the Arg-196 and Arg-217 mutant proteins, and the Lys-282 and Arg-288 double mutant proteins, cross-peaks of F164, I165, C168, L191, V193, S194, G201, V204, S206, A208 and E210, cross-peaks of F161, D162, A163, K190, C192, S194, E213, G246, L289, S294 and L295, and cross-peaks of K256, Y257, F264, S266, R269, F270, I271, D275, T277, C280, T281, S283, F285, T287, L289 and K291 disappeared in the original positions of the MyD88-TIR wild-type, respectively (Ohnishi et al., 2010). However, in most cases, cross-peaks could be found very close to the original positions, which are presumably from the corresponding residues (Fig. 4A). In the spectrum of the R217A mutant, the G201 cross-peak does not appear; it exists at the same position as that of the wild-type but with lower intensity than the threshold used to generate the figure. These residues are mapped onto the structures of MyD88-TIR

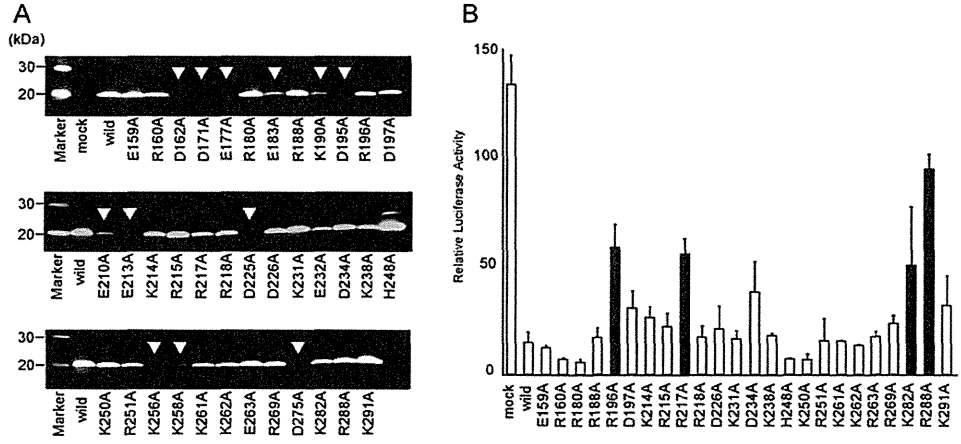

Fig. 3. Functional assay for MyD88-TIR in TLR1/TLR2 signaling. (A) Evaluation of the expression levels of all of the alanine-substituted mutant proteins containing MyD88-TIR in HEK293 cells. Arrowheads indicate mutants with poor expression levels. The expression levels of D162A, D171A, E177A, E183A, K190A, D195A, E210A, E213A, D225A, K256A, K258A and D275A were significantly lower than those of the other mutants. (B) NF-κB reporter gene assay with Pam3CSK4-induced (0.1 μg/ml) 293-hTLR1/2 cells. In this graph, each column indicates the relative luciferase activity of the stimulated cells over the non-stimulated cells. Data represent the mean + S.D. of triplicate wells. This experiment is representative of at least three independent experiments. Black bars indicate the significantly increased NF-κB activity, as compared with the wild-type group. The statistical significance of the differences in the luciferase activities between the wild-type and mutants was analyzed using Dunnett's multiple comparison test. Statistical significance was assumed to be $P < 0.05$.

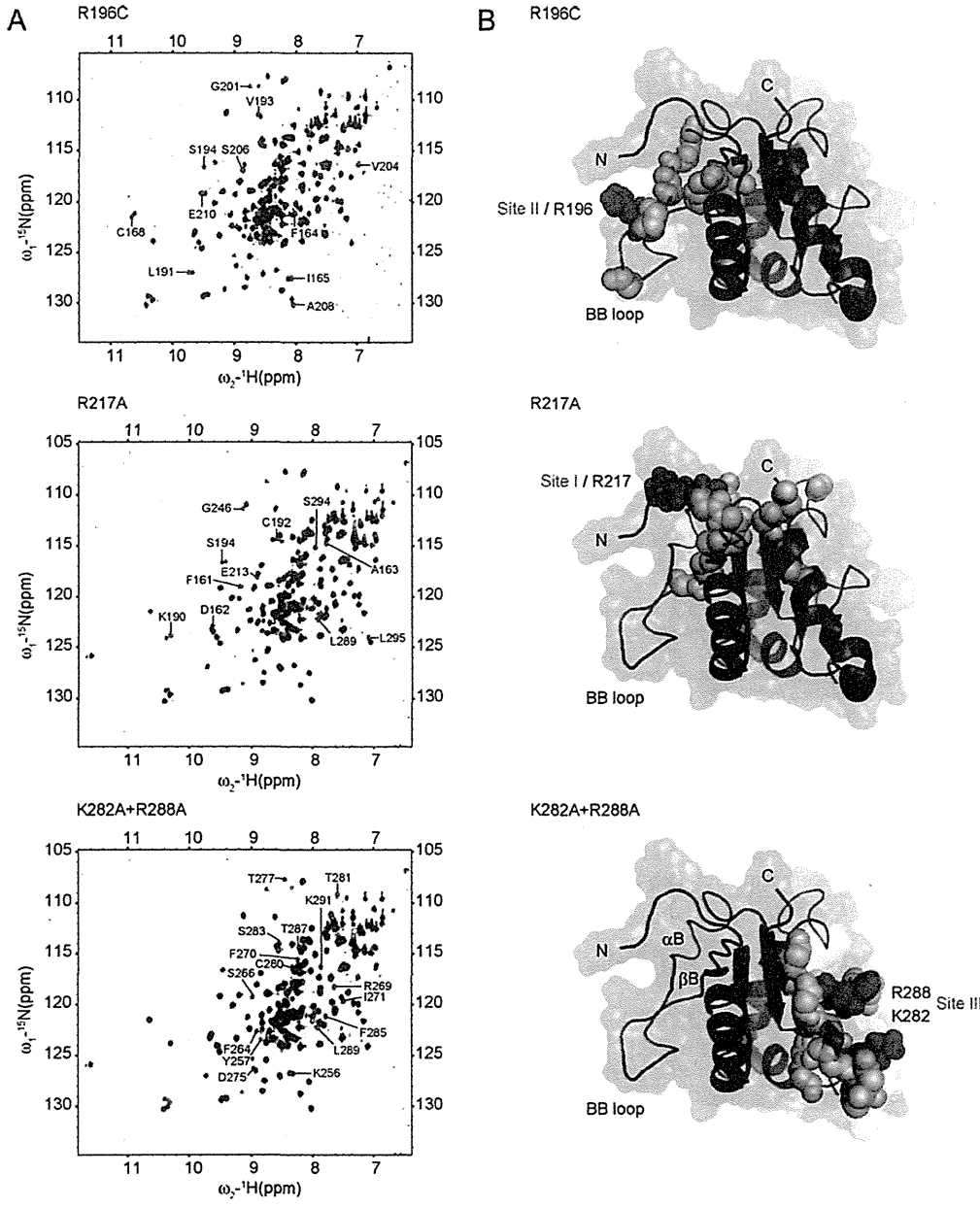

Fig. 4. ^{1}H–^{15}N correlation NMR spectra of MyD88-TIR. (A) Superimposition of ^{1}H–^{15}N correlation NMR spectra for the wild-type MyD88-TIR (red) and mutants (blue). The residues for which the cross-peaks disappeared in the original position of the wild-type MyD88-TIR in the 2D ^{1}H–^{15}N correlation spectra of the mutant proteins are indicated. (B) Structure of the MyD88-TIR (PDB ID: 2z5v) onto which Site I (Arg-217), II (Arg-196), III (Lys-282 and Arg-288) (red), and the residues for which the cross-peaks disappeared in the original position of the wild-type MyD88-TIR in the spectra of the mutant proteins (light brown) are mapped; these residues reside close to each mutated residues (Arg-196, Arg-217, Lys-282, or Arg-288). (For interpretation of the references to color in this figure legend, the reader is referred to the web version of this article.)

(Fig. 4B). The ribbon diagrams of MyD88-TIR structure were generated using the program PyMOL. Additionally, we also performed mutational analysis of MyD88 using a NF-κB luciferase reporter gene activity assay with HEK293T cells transfected with plasmids encoding full-length MyD88. For this assay, we created full-length MyD88 mutants for Sites I-III (R196C, R217A, and K282A/R288A). As shown in Fig. 5A, expression of the full-length MyD88 wild-type in HEK293T cells led to a strong, ligand-independent induction of the NF-κB-dependent luciferase reporter gene. In contrast, expression of the MyD88 mutants, especially R196C and K282A/R288A, led to a significantly reduced induction of the NF-κB-dependent luciferase reporter gene. This result suggests that Sites I, II, and III contribute to interfaces with molecules involved in MyD88 dependent signaling. Among those residues that form Sites I, II, and III, Arg-196 (which forms Site II) has recently been found to be mutated to cysteine in MyD88-deficiency primary immunodeficiency patients (von Bernuth et al., 2008). Hence, we analyzed the effect of cysteine substitution of Arg-196 on interaction with the TLR2-TIR using the GST pull-down assay. In this assay, TLR2-TIR was pulled down by the wild-type MyD88-TIR. Interestingly, the Arg-196 substitution by cysteine resulted in a significant decrease in MyD88-TIR affinity for the TLR2-TIR (Fig. 5B). GST pull-down assays were also conducted to analyze the effects of incorporating an alanine substitution of Arg-217 and a double alanine substitution of Lys-282 and Arg-288 (which form Site I and Site III of the MyD88-TIR, respectively) on interactions with the TLR2-TIR. In these assays, the

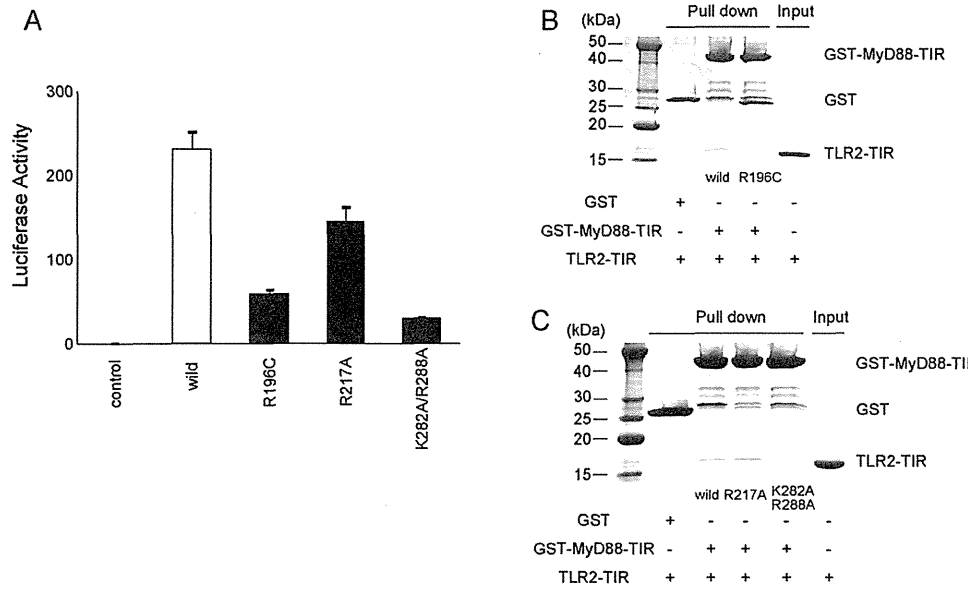

Fig. 5. Functional assay for full-length MyD88 and binding assays for MyD88-TIR mutants with TLR2-TIR. (A) Mutational analysis of MyD88 derived from transfection of HEK293T cells with plasmids encoding the full-length MyD88. Data are shown as the mean + S.D. of quadruplicate wells. Black bars indicate the significantly decreased NF-κB activity, as compared with the wild-type group. The statistical significance of the differences in the luciferase activities between the wild-type and mutants was analyzed using Dunnett's multiple comparison test. Statistical significance was assumed to be $P < 0.05$. (B) Binding assays for wild-type or mutant MyD88-TIRs with TLR2-TIR using GST pull-down assays. The cysteine substitution of Arg-196, which forms Site II, caused a reduced interaction with the TLR2-TIR. (C) The double alanine substitution of Lys-282 and Arg-288, which forms Site III, caused a reduced interaction with TLR2-TIR. The alanine substitution of Arg-217, which forms Site I, had no significant effect.

alanine substitution of Arg-217 had no significant effect. In contrast, the double alanine substitution of Lys-282 and Arg-288 resulted in a significant decrease in MyD88-TIR affinity for the TLR2-TIR (Fig. 5C). These results suggested, therefore, that Site II and Site III, but not Site I, contribute to the interface with TLR2-TIR, as well as with Mal-TIR.

3.4. Similar kinetics of interaction between MyD88, Mal, and TLR2

The binding mode of the TIR domains of MyD88, Mal, TLR1 and TLR2 was analyzed as indicated above (Section 3.1). In addition, we showed that Site II and Site III of the MyD88-TIR served as the binding sites for TLR2-TIR. These two sites also served as binding sites for Mal-TIR in our previous study (Ohnishi et al., 2009). Thus, the present study shows that Site II and Site III of MyD88-TIR form shared binding sites for both TLR2-TIR and Mal-TIR. To analyze mechanisms for the interaction of these TIR proteins, we next evaluated the time-dependent interaction between MyD88, Mal and TLR2 after stimulation with Pam3CSK4 using immunoprecipitation assays. Negative controls consisted of lysates from HEK293T cells, in which expression of TLR2 was not detected, co-transfected with the pcDNA3.1+ myc-tagged MyD88 and pFLAG-CMV6a Mal and stimulated with 0.1 μg/ml Pam3CSK4 for 15 min. In these experiments, stimulation induced the binding activity of MyD88 to TLR2. The binding activity was most significantly enhanced at 30 min post-stimulation. Similarly, the stimulation-induced binding activity of Mal to TLR2 was most significantly enhanced at 15–30 min post-stimulation (Fig. 6). Consequently, these experiments showed that both MyD88 and Mal interacted with TLR2, with the maximal effect occurring 15–30 min after stimulation; this result suggests that these proteins share similar interaction kinetics.

4. Discussion

TIR domains are important signaling modules in TLRs and IL-1/IL-18 signaling events. A TIR domain is typically composed of 135–160 amino acid residues, with the sequence conservation within the domain ranging from 20 to 30%. While the hydrophobic core residues are conserved, the surface exposed residues vary greatly between TIR domains. Consequently, distribution of surface electrostatic potential differs significantly between TIR domains (Dunne et al., 2003), which possibly underlies differences in the binding specificities. Furthermore, recent structural analyses of TIR domain proteins have revealed that the structure of the BB loop, which is considered a functionally important region of TIR domains, differs significantly between TIR domains (Nyman et al., 2008; Ohnishi et al., 2009; Valkov et al., 2011; Xu et al., 2000), suggesting

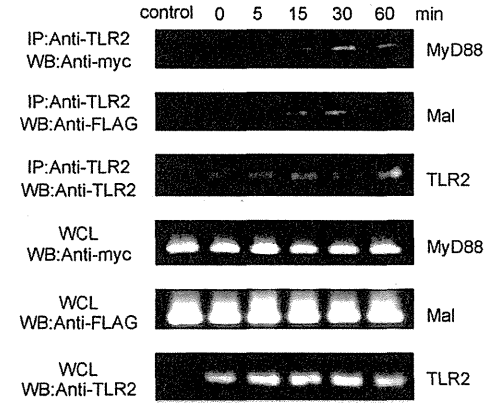

Fig. 6. Time-dependent interaction between MyD88, Mal and TLR2, post-stimulation. The 293-hTLR1/2 cells co-transfected with the pcDNA3.1+ myc-tagged MyD88 and pFLAG-CMV6a Mal were stimulated with 0.1 μg/ml Pam3CSK4 for the indicated intervals. The cell lysates were immunoprecipitated and western blotted. As a negative control, we used lysates from HEK293T cells co-transfected with the pcDNA3.1+ myc-tagged MyD88 and pFLAG-CMV6a Mal and stimulated with 0.1 μg/ml Pam3CSK4 for 15 min. Stimulation with Pam3CSK4 induced the binding activity of MyD88 to TLR2; this activity was most significantly enhanced at 30 min post-stimulation. Similarly, stimulation induced the binding activity of Mal to TLR2, which was most significantly enhanced at 15–30 min post-stimulation.

that the structural deviation of the BB loop might reflect different specificities of the TIR–TIR interaction. Several homotypic interactions have been observed in crystals of TIR domains (Bernoux et al., 2011; Chan et al., 2009; Khan et al., 2004; Tao et al., 2002; Valkov et al., 2011), but heterotypic interactions between TIR–TIR domains have not yet been explained.

We analyzed direct interactions between TIR domains involved in TLR2 signaling using the GST pull-down assay. Mal-TIR directly bound to the TIR domains of receptors (TLR1, TLR2) and MyD88, as well as to TLR4-TIR. In contrast, MyD88-TIR directly bound to the cytosolic TIR domains of TLR1, TLR2, and Mal, but not to TLR4-TIR (Ohnishi et al., 2009) (Fig. 2). These findings are consistent with a previous observation revealed by yeast two-hybrid experiments and GST pull-down assays (Kenny et al., 2009). Thus, these results suggest that hetero-oligomeric TIR–TIR formation between TLR1, TLR2, and adaptors (MyD88 and Mal) is different from that between TLR4 and the same adaptors.

We also identified that three functional surface sites (Sites I–III) of the MyD88-TIR were also important for the Pam3CSK4-activated TLR1/TLR2 signaling pathway, as well as for TLR4 signaling pathway. The alanine substitution of Asp-197, which we previously found to be the functional residue for TLR4 signaling pathway (Ohnishi et al., 2009), resulted in a moderate, but not significant, reduced inhibitory effect in the Pam3CSK4-induced luciferase activity. This indicates that Asp-197 is also likely to be involved in interactions during TLR2 signaling pathway as well as TLR4 signaling pathway (Fig. 3B).

Furthermore, we showed that Sites I, II, and III contributed to interfaces with molecules involved in MyD88 dependent signaling; two of these three functional surface sites, Site II and Site III, served as the binding sites for TLR2-TIR (Fig. 5A–C). Amino acid substitutions may cause unintended global changes in the three-dimensional structures of proteins that can lead to inappropriate conclusions. Therefore, we also examined the purified recombinant proteins using NMR spectroscopy to ensure that no misfolding or global re-arrangements of TIR domains had occurred (Fig. 4A). The residues for which the cross-peaks disappeared in the original position of the wild-type MyD88-TIR in the 2D ^{1}H–^{15}N correlation spectra of the mutant proteins reside close to Arg-196, Arg-217, Lys-282, or Arg-288 (Fig. 4B). This indicates that introduction of the mutations did not affect the overall folding of the domain structures. Interestingly, the two sites have also served as the binding sites for Mal-TIR in our previous study (Ohnishi et al., 2009). Thus, the present study shows that Site II and Site III of MyD88-TIR serve as shared binding sites for both TLR2-TIR and Mal-TIR. Arg-217 in Site I played a crucial role in the TLR2-mediated cellular response to Pam3CSK4 stimulation, but was not involved in direct binding to TLR2. This site has also not been involved in direct binding to Mal-TIR, and the direct interaction of MyD88-TIR with the death domain of IRAK4 was not observed in our previous study (Ohnishi et al., 2009). We demonstrated that the alanine substitution of Arg-217 resulted in no significant decrease in MyD88-TIR affinity for the TLR1-TIR (data not shown). Therefore, Site I may have no involvement in, or make minimal contributions to, interfaces with the TIR domains in TLR1/TLR2 signaling.

We next investigated the time-dependent interaction between MyD88, Mal and TLR2 post-stimulation. This experiment showed that the interaction kinetics of TLR2 with MyD88 was similar to that observed for Mal (Fig. 6). Therefore, it is possible that MyD88 and Mal bind to identical or different TLR2 molecules and share similar interaction kinetics. The crystal structure of the MyD88-IRAK4-IRAK2 death domain complex has recently been reported (Lin et al., 2010). The structure reveals a helical oligomer (called a Myddosome), which consists of six MyD88, four IRAK-4 and four IRAK-2 death domains. As this structure, an unknown complicated assembly of the TIR domains, including MyD88, Mal, TLR1, and TLR2, may form the higher order oligomer.

Primary immuno-deficiency syndromes with innate immune defects have recently been defined (Notarangelo et al., 2009). The phenotypes characteristic of IRAK-4 deficiency and MyD88 deficiency suggest that the Gram-positive bacterial recognition system is dependent on the TLR2/Mal/MyD88/IRAK-4 signaling cascade, indicating that it is important to consider the links between protein functions and gene mutations in the TLR2 signaling pathway. Most gene variations in IRAK-4 deficiency and MyD88 deficiency cause the loss of stability of proteins or the deletion of proteins (Conway et al., 2010; Ku et al., 2007; von Bernuth et al., 2008). We focused on the Site II residue, Arg196 of MyD88, which has been found to be mutated to cysteine in MyD88 deficiency patients (von Bernuth et al., 2008). The 2D ^{1}H–^{15}N correlation spectrum showed that the residues for which the cross-peaks were shifted by the cysteine substitution at Arg-196 reside close to Arg-196. In these residues, F164, I165, C168 are all located distant in the sequence, but proximal in space to Arg-196 (Fig. 4B). This indicates that introduction of the mutation did not affect the overall folding of the domain structure, although it would be expected to exert a minor effect on the BB loop that connects the second β-strand and second helix and consists of residues 194–208, owing to its proximity. Consequently, the Arg-196 substitution did not cause destabilization of the MyD88-TIR protein. However, this missense mutation caused a significant decrease in the direct binding ability to TLR2-TIR as well as to Mal-TIR (Fig. 4A) (Ohnishi et al., 2009). The loss of interactions of MyD88-TIR with TLR2-TIR or Mal-TIR caused by the mutation would be a critical molecular factor influencing the specific phenotype of MyD88 deficiency patients. Thus, this result may provide a molecular explanation of the symptoms experienced by MyD88 deficiency patients.

In conclusion, we have demonstrated that MyD88-TIR directly binds to TLR2-TIR, but not to TLR4-TIR. We have also shown that two isolated sites in the MyD88-TIR mediate direct interactions with TLR2-TIR and that these sites are shared with Mal-TIR. The interaction kinetics for TLR2 with MyD88 is similar to TLR2 with Mal. Identification of the MyD88 residues that are involved in direct interactions with TLR2 is of clinical significance because of the association of one of these residues with primary immunodeficiency syndrome. The mechanism of TLR2 signaling initiation remains to be clarified by further studies. However, we believe that the novel information on the binding mode of the TIR proteins provided by this study will facilitate future structural determination of hetero-oligomeric TIR domain complexes.

Acknowledgments

We thank Dr. Tokumi, T., Souma, W., Tsuji, K., and Kasahara, K. for their technical help. This work was supported by Grants-in-Aid for Scientific Research from the Ministry of Education, Culture, Sports, Science and Technology of Japan and by Health and Labour Science Research Grants for Research on Intractable Diseases from the Ministry of Health, Labour and Welfare.

Appendix A. Supplementary data

Supplementary data associated with this article can be found, in the online version, at http://dx.doi.org/10.1016/j.molimm.2012.05.003.

References

Akira, S., Uematsu, S., Takeuchi, O., 2006. Pathogen recognition and innate immunity. Cell 124, 783–801.

Arbour, N.C., Lorenz, E., Schutte, B.C., Zabner, J., Kline, J.N., Jones, M., Frees, K., Watt, J.L., Schwartz, D.A., 2000. TLR4 mutations are associated with endotoxin hyporesponsiveness in humans. Nature Genetics 25, 187–191.

Bernoux, M., Ve, T., Williams, S., Warren, C., Hatters, D., Valkov, E., Zhang, X., Ellis, J.G., Kobe, B., Dodds, P.N., 2011. Structural and functional analysis of a plant resistance protein TIR domain reveals interfaces for self-association, signaling, and autoregulation. Cell Host Microbe 9, 200–211.

Chan, S.L., Low, L.Y., Hsu, S., Li, S., Liu, T., Santelli, E., Negrate, G.L., Reed, J.C., Woods Jr., V.L., Pascual, J., 2009. Molecular mimicry in innate immunity: crystal structure of a bacterial TIR domain. Journal of Biological Chemistry 284, 21386–21392.

Conway, D.H., Dara, J., Bagashev, A., Sullivan, K.E., 2010. Myeloid differentiation primary response gene 88 (MyD88) deficiency in a large kindred. Journal of Allergy and Clinical Immunology 126, 172–175.

Delaglio, F., Grzesiek, S., Vuister, G., Zhu, G., Pfeifer, J., Bax, A., 1995. NMRPipe: a multidimensional spectral processing system based on UNIX pipes. Journal of Biomolecular NMR 6, 277–293.

Dunne, A., Ejdeback, M., Ludidi, P.L., O'Neill, L.A.J., Gay, N.J., 2003. Structural complementarity of Toll/interleukin-1 receptor domain in Toll-like receptors and the adaptors Mal and MyD88. Journal of Biological Chemistry 278, 41443–41451.

Goddard, T.D., Kneller, D.G., 1999. SPARKY 3. University of California, San Francisco.

Guan, Y., Ranoa, D.R.E., Jiang, S., Mutha, S.K., Li, X., Baudry, J., Tapping, R.I., 2010. Human TLRs10 and 1 share common mechanisms of innate immune sensing but not signaling. Journal of Immunology 184, 5094–5103.

Horng, T., Barton, G.M., Flavell, R.A., Medzhitov, R., 2002. The adaptor molecule TIRAP provides signaling specificity for Toll-like receptors. Nature 420, 329–333.

Kagan, J.C., Medzhitov, R., 2006. Phosphoinositide-mediated adaptor recruitment controls Toll-like receptor signaling. Cell 125, 943–955.

Kaisho, T., Akira, S., 2006. Toll-like receptor function and signaling. Journal of Allergy and Clinical Immunology 117, 979–987.

Kawai, T., Akira, S., 2007. Signaling to NF-κB by Toll-like receptors. Trends in Molecular Medicine 13, 460–469.

Kenny, E.F., Talbot, S., Gong, M., Golenbock, D.T., Bryant, C.E., O'Neill, L.A.J., 2009. MyD88 adaptor-like is not essential for TLR2 signaling and inhibits signaling by TLR3. Journal of Immunology 183, 3642–3651.

Khan, J.A., Brint, E.K., O'Neill, L.A.J., Tong, L., 2004. Crystal structure of the Toll/interleukin-1 receptor domain of human IL-1RAPL. Journal of Biological Chemistry 279, 31664–31670.

Khor, C.C., Chapman, S.J., Vannberg, F.O., Dunne, A., Murphy, C., Ling, E.Y., Frodsham, A.J., Walley, A.J., Kyrieleis, O., Khan, A., Aucan, C., Segal, S., Moore, C.E., Knox, K., Campbell, S.J., Lienhardt, C., Scott, A., Aaby, P., Sow, O.Y., Grignani, R.T., Sillah, J., Sirugo, G., Peshu, N., Williams, T.N., Maitland, K., Davies, R.J.O., Kwiatkowski, D.P., Day, N.P., Yala, D., Crook, D.W., Marsh, K., Berkley, J.A., O'Neill, L.A.J., Hill, A.V.S., 2007. A Mal functional variant is associated with protection against invasive pneumococcal disease, bacteremia, malaria and tuberculosis. Nature Genetics 39, 523–528.

Ku, C.L., von Bernuth, H., Picard, C., Zhang, S.Y., Chang, H.H., Yang, K., Chrabieh, M., Issekutz, A.C., Cunningham, C.K., Gallin, J., Holland, S.M., Roifman, C., Ehl, S., Smart, J., Tang, M., Barrat, F.J., Levy, O., McDonald, D., Day-Good, N.K., Miller, R., Takada, H., Hara, T., Al-Hajjar, S., Al-Ghonaium, A., Speert, D., Sanlavillle, D., Li, X., Geissmann, F., Vivier, E., Maródi, L., Garty, B.Z., Chapel, H., Rodriguez-Gallego, C., Bossuyt, X., Abel, L., Puel, A., Casanova, J.L., 2007. Selective predisposition to bacterial infections in IRAK-4-dedicient children: IRAK-4-dependent TLRs are otherwise redundant in protective immunity. Journal of Experimental Medicine 204, 2407–2422.

Lin, S.C., Lo, Y.C., Wu, H., 2010. Helical assembly in the MyD88-IRAK4-IRAK2 complex in TLR/IL-1R signaling. Nature 465, 885–890.

Notarangelo, L.D., Fischer, A., Geha, R.S., Casanova, J.L., Chapel, H., Conley, M.E., Cunningham-Rundles, C., Etzioni, A., Hammartröm, L., Nonoyama, S., Ochs, H.D., Puck, J., Roifman, C., Seger, R., Wedgwood, J., 2009. Primary immunodefiencies: 2009 update. Journal of Allergy and Clinical Immunology 124, 1161–1178.

Nyman, T., Stenmark, P., Flodin, S., Johansson, I., Hammarstrm, M., Nordlund, P., 2008. The crystal structure of the human Toll-like receptor 10 cytoplasmic domain reveals a putative signaling dimer. Journal of Biological Chemistry 283, 11861–11865.

Ohnishi, H., Tochio, H., Kato, Z., Orii, K.E., Li, A., Kimura, T., Hiroaki, H., Kondo, N., Shirakawa, M., 2009. Structual basis for the multiple interaction of the MyD88 TIR domain in TLR4 signaling. Proceedings of the National Academy of Sciences of the United States of America 106, 10260–10265.

Ohnishi, H., Tochio, H., Kato, Z., Kimura, T., Hiroaki, H., Kondo, N., Shirakawa, M., 2010. 1H, 13C, and 15N resonance assignment of the TIR domain of human MyD88. Biomolecular NMR Assignments 2, 123–125.

O'Neill, L.A., Bowie, A.G., 2007. The family of five: TIR-domain-containing adaptors in Toll-like receptor signaling. Nature Reviews Immunology 7, 353–364.

Picard, C., Casanova, J.L., Puel, A., 2011. Infectious disease in patients with IRAK-4, MyD88, NEMO, or IκBα deficiency. Clinical Microbiology Reviews 24, 490–497.

Santos-Sierra, S., Deshmukh, S.D., Kalnitski, J., Küenzi, P., Wymann, M.P., Golenbock, D.T., Hanneke, P., 2009. Mal connects TLR2 to PI3Kinase activation and phagocyte polarization. EMBO Journal 28, 2018–2027.

Schanda, P., Brutscher, B., 2005. Very fast two-dimensional NMR spectroscopy for real-time investigation of dynamic events in proteins on the time scale of seconds. Journal of the American Chemical Society 127, 8014–8015.

Tao, X., Xu, Y., Zheng, Y., Beg, A.A., Tong, L., 2002. An extensively associated dimer in the structure of the C713S mutant of the TIR domain of human TLR2. Biochemical and Biophysical Research Communications 299, 216–221.

Tao, X., Tong, L., 2009. Expression, purification, and crystallization of Toll/interleukin-1 receptor (TIR) domains. Methods in Molecular Biology 517, 81–88.

Ulrichts, P., Peelman, F., Beyaert, R., Tavernier, J., 2007. MAPPIT analysis of TLR adaptor complexes. FEBS Letters 581, 629–636.

Valkov, E., Stamp, A., DiMaio, F., Baker, D., Verstak, B., Roversi, P., Kellie, S., Sweet, M.J., Mansell, A., Gay, N.J., Martin, J.L., Kobe, B., 2011. Crystal structure of Toll-like receptor adaptor MAL/TIRAP reveals the molecular basis for signal transduction and disease protection. Proceedings of the National Academy of Sciences of the United States of America 108, 14879–14884.

von Bernuth, H., Picard, C., Jin, Z., Pankla, R., Xiao, H., Ku, C.L., Chrabieh, M., Mustapha, I.B., Ghandil, P., Camcioglu, Y., Vasconcelos, J., Sirvent, N., Guedes, M., Vitor, A.B., Herrero-Mata, M.J., Aróstegui, J.I., Rodrigo, C., Alsina, L., Ruiz-Ortiz, E., Juan, M., Fortuny, C., Yagüe, J., Antón, J., Pascal, M., Chang, H.H., Janniere, L., Rose, Y., Garty, B.Z., Chapel, H., Issekutz, A., Maródi, L., Rodriguez-Gallego, C., Banchereau, J., Abel, L., Li, X., Chaussabel, D., Puel, A., Casanova, J.L., 2008. Pyogenic bacterial infections in humans with MyD88 deficiency. Science 321, 691–696.

Xu, Y., Tao, X., Shen, B., Horng, T., Medzhitov, R., Manley, J.L., Tong, L., 2000. Structural basis for signal transduction by the Toll/interleukin-1 receptor domains. Nature 408, 111–115.

ORIGINAL ARTICLE

Risk Factors for Infantile Atopic Dermatitis and Recurrent Wheezing

N Kawamoto,[1,2] T Fukao,[1] H Kaneko,[1,3] K Hirayama,[1] S Sakurai,[1] T Arai,[1] M Kondo,[1] M Kawamoto,[1] E Matsui,[1] T Teramoto,[1] K Kasahara,[1] C Bai,[1] G Zhang,[1] K Omoya,[1] E Matsukuma,[1] M Morimoto,[2] H Suzuki,[1] Y Aoki,[1] T Kimura,[2] M Nada,[1] H Morita,[3] T Tokumi,[1] M Takemura,[4] M Seishima,[4] M Shiraki,[5] S Iwasa,[5] N Kondo[1]

[1]Department of Pediatrics, Graduate School of Medicine, Gifu University, Gifu, Japan
[2]Neonatal Intensive Care Unit, Gifu University Hospital, Gifu, Japan
[3]Department of Clinical Research, National Hospital Organization, Nagara Medical Center, Gifu, Japan
[4]Department of Informative Clinical Medicine, Graduate School of Medicine, Gifu University, Gifu, Japan
[5]Iwasa Maternity, Gifu, Japan

Abstract

Background: The pathogenic mechanisms of atopic dermatitis (AD) and recurrent wheezing (RW) during infancy are not fully understood.
Objective: We evaluated immunological markers associated with AD and RW during infancy.
Methods: We followed a cohort (n=314) from birth to 14 months of age. Some of the participants underwent a physical examination and blood test at 6 and 14 months of age. Univariate and multivariate logistic regression analysis and receiver operating characteristic curve analysis were performed to find which immunological markers could be risk factors for AD and RW.
Results: Of 16 immunological markers found in cord blood, only immunoglobulin (Ig) E was associated with AD at 6 months of age (adjusted OR [aOR], 1.607). None of the markers was associated with AD or RW at 14 months of age. Of 23 immunological markers at 6 months of age, total IgE (aOR, 1.018) and sensitization to egg white (aOR, 23.246) were associated with AD at 14 months of age. Phytohemagglutinin (PHA)–induced production of interleukin (IL) 4 from peripheral blood mononuclear cells (PBMCs) (aOR, 1.043) was associated with RW at 14 months of age.
Conclusion: Cord blood IgE was a risk factor for AD at 6 months of age. Total IgE and sensitization to egg white at 6 months of age were risk factors for AD at 14 months of age. PHA-induced IL-4 production in PBMCs at 6 months of age was a risk factor for RW at 14 months of age.

Key words: Birth cohort. Infants. Cord blood. Atopic dermatitis. Recurrent wheezing.

Resumen

Antecedentes: Los mecanismos patógenos de la dermatitis atópica (DA) y las sibilancias recurrentes (SR) durante el primer año de vida no se conocen completamente.
Objetivo: Se evaluaron los factores inmunológicos asociados a DA y SR durante el primer año de vida.
Métodos: Se realizó el seguimiento de una cohorte (n = 314) desde el nacimiento hasta los 14 meses de edad. Algunos de los participantes se sometieron a una exploración física y a un análisis de sangre a los 6 y a los 14 meses de edad. Se realizaron análisis de regresión logística unifactoriales y multifactoriales y análisis de la curva de eficacia diagnóstica para determinar qué factores inmunológicos podrían ser factores de riesgo para la DA y las SR.
Resultados: De 16 factores inmunológicos hallados en la sangre del cordón umbilical, solo la inmunoglobulina E (IgE) se asoció a DA a los 6 meses de edad (oportunidad relativa ajustada [ORa], 1,607). Ninguno de los factores se asoció a DA o SR a los 14 meses de edad. De 23 factores inmunológicos a los 6 meses de edad, el total de IgE (ORa, 1,018) y la sensibilización a la clara de huevo (ORa, 23,246) se asociaron a DA a los 14 meses de edad. La producción de interleucina (IL) 4 inducida por fitohemaglutinina (FHA) de las células mononucleares de sangre periférica (CMSP) (ORa, 1,043) se asoció a SR a los 14 meses de edad.
Conclusión: La presencia de IgE en la sangre del cordón umbilical fue un factor de riesgo de DA a los 6 meses de edad. El total de IgE y la sensibilización a la clara de huevo a los 6 meses de edad fueron factores de riesgo de DA a los 14 meses de edad. La producción de IL-4 inducida por FHA en las CMSP a los 6 meses de edad fue un factor de riesgo de SR a los 14 meses de edad.

Palabras clave: Cohorte de nacimiento. Lactantes. Sangre del cordón umbilical. Dermatitis atópica. Sibilancias recurrentes.

Introduction

Allergic diseases such as atopic dermatitis (AD), asthma, and food allergy are common diseases in children. AD is the most common allergic disease during infancy, and onset occurs during the first 6 months of life in 45% of those affected [1]. Recurrent wheezing (RW) is also an important problem during the first few years of life, because some children with RW develop bronchial asthma [2]. Genetic factors [3] and environmental factors [4] affect the development of allergic diseases. The role of genetic factors has been reported by our group [5,6] and by other authors [7]. We also reported on the role of cord blood factors associated with allergic diseases [8-10]. However, the pathogenic mechanisms of these diseases are still not fully understood.

Immunoglobulin (Ig) E and eosinophils are considered markers of allergic disease in early childhood [11,12]. Today, several new immunological markers have been investigated. Helper T cell (T_H) imbalance is considered to be associated with allergic diseases [13]. Type 2 T_H cells (T_H2), which produce cytokines such as interleukin (IL) 4, IL-5, and IL-13 promote secretion of IgE and differentiation of eosinophils and dominate T-cell responses in allergic diseases [14]. T_H1 cells, which produce IL-2, IL-12, and interferon (IFN) γ, confer immunity against infection and suppress T_H2 cells [14]. Several studies have reported the importance of regulatory pathways, such as regulatory T cells (Treg), IL-10, and transforming growth factor ß [14,15]. However, the question as to which immunological markers really affect allergic disease in early childhood remains unclear.

We have been performing a cohort study (the Gifu Allergy and Immunology Cohort Study [GAICS]) since 2004. To our knowledge, few birth cohort studies have examined immunological changes during infancy. We describe some of the immunological markers of cord blood and peripheral blood at 6 and 14 months of age and study their role in AD and RW.

Methods

Study Participants and Design

We performed this analysis as a part of the GAICS, which included 314 infants born in a maternity hospital from October 2004 to July 2005. The details of the study were explained to the parent(s) before birth. Informed consent was obtained from all the parent(s). Cord blood samples were taken at birth. All participants were followed up using questionnaires at birth and at 6 and 14 months of age.

In order to analyze the immunological markers of allergic diseases, more than half of the participants were recruited to a group in which the participants underwent further tests, including a physical examination by a pediatric allergist and blood sampling (previous written agreement from the parent[s]). All the questionnaires were completed. The remaining participants were followed up by questionnaire only and will be analyzed in future papers. All parts of this cohort study were approved by the Ethics Committee of the Graduate School of Medicine, Gifu University, Gifu, Japan.

Diagnosis

AD was diagnosed by a pediatric allergist according to Hanifin and Rajka's minor criteria [11]; RW was diagnosed by a pediatric allergist based on a history of more than 2 episodes of physician-diagnosed wheezing.

Laboratory Determinations

Total white blood cell (WBC) counts were performed using an automated instrument. Blood smears from peripheral blood samples were stained (Wright-Giemsa), and a white blood cell differential test was performed. Absolute eosinophil and basophil counts were calculated from total WBC numbers.

Cord blood and peripheral blood serum IgE were examined using LUMIPULSE IgE (Fujirebio Inc). Specific IgE was measured using the radioallergosorbent test, and sensitization was defined as a specific IgE concentration >0.34 U/mL for certain allergens (egg white, cow's milk, wheat, soy bean, house dust [h1], *Dermatophagoides farinae*, dog dander, and cat dander). Cord blood serum IgA was analyzed to evaluate the contamination of maternal blood, and samples of that IgA ≥1 mg/dL were excluded [16].

Flow Cytometry of Lymphocyte Subpopulations

Flow cytometry was performed on a Cytomics FC500 device (Beckman Coulter). Whole blood samples were stained with CD3, CD19, CD4, CD8, CD56/CD16, and CD4/CD25 antibodies (Beckman Coulter). An appropriate amount of fluorescence antibody and 100 μL of whole blood were mixed and incubated for 20 minutes. The whole blood samples were treated with ammonium chloride to lyse the erythrocytes, and the cells were washed twice with phosphate-buffered saline (PBS). The cells were then resuspended in 0.5 mL of PBS and analyzed immediately. The percentages of $CD3^+$, $CD19^+$, and $CD4^+$ cells in the lymphocytes were named, respectively, CD3% (T cell), CD19% (B cell), and CD4% (helper T cell). The $CD8^+$ cells were divided into $CD8^{bright}$ and $CD8^{dull}$. Most of the $CD8^{dull}$ cells expressed CD56 (data not shown) and were considered to be natural killer cells. On the other hand, most of the $CD8^{bright}$ cells expressed CD3, but not CD56 (data not shown). Therefore, the percentages of $CD8^+$ cells and $CD8^{bright}$ and $CD8^{dull}$ in the lymphocytes were named CD8%, $CD8^{bright}$% (cytotoxic T cell), and $CD8^{dull}$% (some of the natural killer cells). The percentages of double-positive CD56 and CD16 cells in the lymphocytes were named $CD56^+CD16^+$%. The percentage of CD56-positive and CD16-negative cells were named $CD56^+CD16^-$%. The $CD25^+$ cells in the $CD4^+$ lymphocytes were named $CD4^+CD25^+$%.

Intracellular Cytokine Analysis

Intracellular cytokine staining was performed as reported elsewhere [17]. A total of 0.5 mL of heparinized whole blood was added to 0.5 mL of an RPMI-1640 medium, incubated with a combination of 25 ng/mL of phorbol myristate acetate (PMA) and 1 μg/mL of ionomycin in the presence of 10 μg/mL of brefeldin A (Sigma), and cultured for 4 hours at 37°C in a humidified atmosphere containing 5% CO_2. Surface staining (CD4, CD8) was carried out at room temperature for 20 minutes in the dark. The blood samples were then

fixed and permeabilized with an IntraPrep Permeabilization Reagent (Beckman Coulter). Finally, the cells were incubated with monoclonal antibodies of anti–IFN-γ fluorescein isothiocyanate (BD Biosciences) or anti–IL-4 phycoerythrin (BD Biosciences) for 40 minutes in the dark and then analyzed using flow cytometry. The percentage of IFN–γ-producing cells in a $CD4^+$ and a $CD8^{bright}$ cell was considered to be T_H1% and cytotoxic T cells (T_C)1%, respectively. The percentage of IL-4–producing cells in a $CD4^+$ and a $CD8^{bright}$ cell was considered to be T_H2% and T_C2%, respectively.

Cell Preparation and Culture

Cord blood mononuclear cells (CBMCs) or peripheral blood mononuclear cells (PBMCs) were isolated by centrifugation on Ficoll/Paque (Pharmacia AB) and washed 3 times. The isolated CBMCs/PBMCs were suspended at a final concentration of 1×10^6 cells/mL in an RPMI 1640 medium supplemented with 10% heat-inactivated fetal calf serum, 2mM L-glutamine, 100 IU/mL of penicillin, and 100 μg/mL of streptomycin. Cell suspensions were cultured in the presence or absence of 10 μg/mL of phytohemagglutinin (PHA) (Gibco BRL) for 24 hours at 37°C in a humidified atmosphere containing 5% CO_2. The culture supernatants were measured using a human IFN-γ enzyme-linked immunosorbent assay (ELISA) kit (Ohtsuka) and an IL-4 US ELISA kit (BioSource). The detection limits of the ELISAs were 15.6-1000 pg/mL (IFN-γ) and 0.39-25.0 pg/mL (IL-4).

Statistics

Multivariate logistic analyses were performed to determine whether there were any cord blood immunological markers that could predict AD at 6 months of age, whether there were any cord or peripheral blood immunological markers at birth or at 6 months of age that could predict AD at 14 months of age, and whether there were any cord or peripheral blood immunological markers at birth or at 6 months of age that could predict RW at 14 months of age.

SPSS version 17.0 (SPSS, Inc) was used for univariate and multivariate logistic regression analysis. Values below the detection limit were allotted half the detection limit. A separate univariate risk factor analysis was conducted for AD at 6 and 14 months of age. To predict AD and RW, we fitted a multiple regression model that included all potential predictors with a univariate P value <.05. A backward stepwise (likelihood ratio) procedure was used to select a final model.

Receiver operating characteristic (ROC) curve analysis was also performed with SPSS version 17.0 to evaluate the predictability of the factors selected in the logistic regression analysis.

Results

Study Participants and Baseline Characteristics

A flowchart of the GAICS is shown in the Figure. Of the 314 participants, 171 (54.5%) were female, mean (SD) gestational age was 278.0 (7.5) days (39 weeks and 5.0 days), and mean birth weight was 3120.5 (388.2) g.

We recruited participants who had undergone physical examination at 6 and 14 months of age (Figure). First, we compared data for participants who had undergone the physical examination and for the remaining participants. No significant differences were observed for gestational age, birth weight, sex, and family history of the parent(s) of patients from both groups (Table 1). The final sample comprised participants who had undergone a physical examination.

Prevalence of Atopic Dermatitis and Recurrent Wheezing

Of the 174 participants who had a physical examination at 6 months of age, 43 (24.7%) and 0 (0.0%) suffered from AD and RW, and were referred to as 6MAD(+) or 6MRW(+), respectively. Those who did not have AD or RW at 6 months of age were referred to as 6MAD(–) and 6MRW(–), respectively. Of the 157 participants who had a physical examination at 14 months of age, 30 (19.1%) and 12 (7.6%) suffered from AD and RW, and were referred to as 14MAD(+) or 14MRW(+), respectively. Those who did not have AD or RW at 14 months of age were named 14MAD(–) and 14MRW(–), respectively. Among the 30 14MAD(+) participants, only 4 also suffered from RW.

Risk Factors for Atopic Dermatitis at 6 Months of Age

We analyzed whether immunological markers in cord blood could be risk factors for 6MAD(+) (Table 2). Univariate logistic regression analysis showed that increases in cord blood

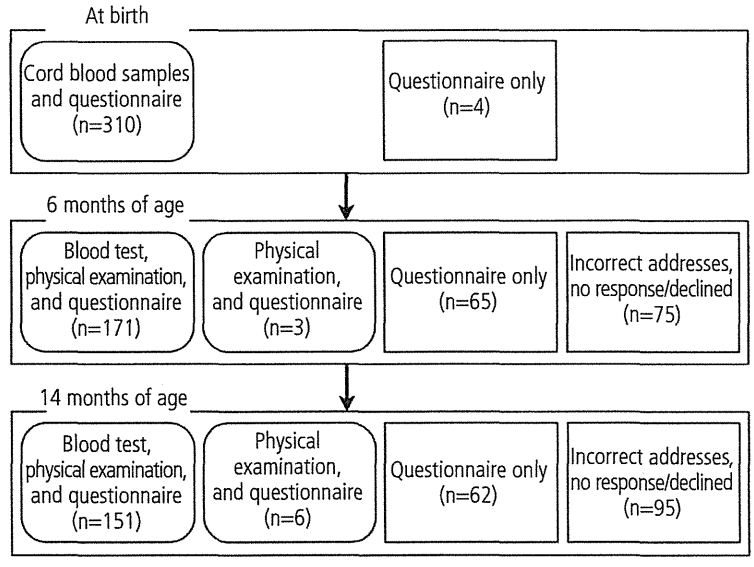

Figure. Flowchart of study participants in the Gifu Allergy and Immunology Cohort Study. For this analysis of immunological markers and physician-diagnosed allergic disease, we used participants who had undergone a physical examination at 6 and 14 months of age (shown as a round-cornered box).

Table 1. Comparison Between Participants Who Underwent a Physical Examination and the Remaining Participants

Physical Examination at 6 Months of Age	Yes	No	*P* Value
Gestational age	278.15 (6.89) d (n=169) 39 wk 5.15 d	277.75 (8.88) d (n=59) 39 wk 4.75 d	NS[a]
Weight at birth	3118.48 (380.28) g (n=173)	3125.95 (411.67) g (n=65)	NS[a]
Male/male+female	81/174 (46.55%)	62/140 (44.29%)	NS[b]
Allergic history			
Father	55/162 (33.95%)	48/123 (39.02%)	NS[b]
Mother	70/164 (42.68%)	58/125 (46.40%)	NS[b]
At least 1 parent	98/162 (60.50%)	78/124 (62.90%)	NS[b]
Both parents	27/162 (16.67%)	28/124 (22.58%)	NS[b]
Physical Examination at 14 Months of Age	**Yes**	**No**	***P* Value**
Gestational age	278.46 (7.10) d (n=148) 39 wk 5.46 d	277.29 (8.01) d (n=80) 39 wk 4.29 d	NS[a]
Weight at birth	3100.68 (404.22) g (n=151)	3154.97 (358.46) g (n=87)	NS[a]
Male/male+female	68/157 (43.31%)	75/157 (47.77%)	NS[b]
Allergic history			
Father	51/144 (35.42%)	52/141 (36.88%)	NS[b]
Mother	66/146 (45.21%)	62/143 (43.36%)	NS[b]
At least 1 parent	91/144 (63.20%)	84/142 (59.86%)	NS[b]
Both parents	26/144 (18.06%)	29/142 (20.42%)	NS[b]

Abbreviation: NS, nonsignificant.
[a]Mann-Whitney test.
[b]Fisher exact test.

Table 2. Odds Ratio (OR) for Having Atopic Dermatitis (AD) at 6 Months of Age According to the Univariate Logistic Regression Analysis of Markers in Cord Blood

	AD 6M (–)		AD 6M (+)		Total				95% CI for OR	
	Mean	(SD)	Mean	(SD)	Mean	(SD)	*P* Value	OR	Lower	Upper
Cord blood										
WBC	12.51	(3.31)	12.21	(4.17)	12.44	(3.53)	.676	0.976	0.872	1.093
Eosinophils	332.4	(186.2)	348.3	(171.3)	336.4	(182.0)	.664	1.000	0.998	1.003
Basophils	78.89	(57.06)	94.03	(76.85)	82.67	(62.63)	.233	1.004	0.998	1.010
IgE	0.54	(0.75)	0.95	(1.42)	0.64	(0.97)	.034	1.462	1.029	2.078
T_H1%	0.25	(0.26)	0.27	(0.21)	0.25	(0.24)	.629	1.439	0.328	6.303
T_H2%	0.17	(0.21)	0.20	(0.23)	0.17	(0.21)	.475	1.833	0.348	9.669
T_C1%	0.60	(0.72)	0.59	(0.62)	0.60	(0.69)	.981	0.994	0.579	1.706
T_C2%	0.03	(0.08)	0.02	(0.07)	0.03	(0.08)	.535	0.148	0.000	61.836
CD3%	51.22	(14.93)	54.75	(16.06)	52.10	(15.24)	.223	1.016	0.991	1.041
CD19%	9.68	(5.57)	8.33	(4.58)	9.35	(5.36)	.184	0.948	0.876	1.026
CD4%	39.92	(11.83)	41.83	(12.22)	40.40	(11.92)	.406	1.014	0.982	1.047
$CD8^{bright}$%	11.62	(4.79)	13.32	(6.36)	12.03	(5.24)	.107	1.060	0.988	1.138
$CD56^+CD16^+$%	9.09	(5.06)	10.05	(6.03)	9.33	(5.31)	.348	1.034	0.964	1.108
$CD56^+CD16^-$%	1.65	(1.21)	1.50	(0.87)	1.61	(1.13)	.504	0.882	0.610	1.275
$CD4^+CD25^+$%	11.62	(2.79)	12.50	(3.07)	11.84	(2.88)	.114	1.108	0.976	1.260
IFN-γ (PHA)	556.6	(961.3)	1111.6	(1883.3)	687.4	(1255.9)	.043	1.000	1.000	1.001
IL-4 (PHA)	5.74	(4.61)	6.13	(4.98)	5.84	(4.69)	.668	1.017	0.941	1.099

Abbreviations: IFN, interferon; Ig, immunoglobulin; IL, interleukin; PHA, phytohemagglutinin; WBC, white blood cells.

IgE levels and PHA-induced IFN-γ production by CBMCs were associated with 6MAD(+).

After stepwise multivariate logistic regression, only cord blood IgE (adjusted OR [aOR]), 1.607; 95% CI, 1.082-2.387; *P*=.019) remained in the model (Table 3).

A ROC curve analysis to evaluate the predictability of cord blood IgE for distinguishing 6MAD(+) from 6MAD(–) revealed the area under the curve (AUC) of cord blood IgE to be 0.564 (95% CI, 0.456-0.672; *P*=.230]. Hence, cord blood IgE is a risk factor but not a predictive factor for AD at 6 months of age.

Table 3. Adjusted Odds Ratio (aOR) for Having Atopic Dermatitis at 6 Months of Age According to Multivariate Logistic Regression Analysis of Markers in Cord Blood

				95% CI for aOR	
		P Value	aOR	Lower	Upper
Cord blood					
Step 1	IgE	.039	1.552	1.022	2.359
	IFN-γ (PHA)	.144	1.000	1.000	1.001
Step 2	IgE	.019	1.607	1.082	2.387

Abbreviations: IFN, interferon; Ig, immunoglobulins; PHA, phytohemagglutinin.

Table 4. Odds Ratio (OR) for Having Atopic Dermatitis (AD) at 14 Months of Age According to Univariate Logistic Regression Analysis of Markers in Cord Blood and at 6 Months

	AD 14M (–)		AD 14M (+)		Total				95% CI for OR	
	Mean	(SD)	Mean	(SD)	Mean	(SD)	*P* Value	OR	Lower	Upper
Cord blood										
WBC	12.22	(3.40)	12.58	(4.18)	12.30	(3.58)	.646	1.028	0.912	1.160
Eosinophils	314.8	(180.8)	342.2	(182.4)	321.2	(180.8)	.489	1.001	0.998	1.003
Basophils	72.15	(52.99)	92.81	(74.04)	76.87	(58.77)	.118	1.005	0.999	1.012
IgE	0.54	(0.81)	0.60	(0.56)	0.55	(0.76)	.684	1.107	0.679	1.805
T_H1%	0.25	(0.26)	0.31	(0.29)	0.26	(0.27)	.284	2.205	0.519	9.370
T_H2%	0.20	(0.24)	0.16	(0.15)	0.19	(0.23)	.394	0.404	0.050	3.249
T_C1%	0.58	(0.71)	0.58	(0.62)	0.58	(0.69)	.991	1.003	0.552	1.825
T_C2%	0.03	(0.04)	0.04	(0.14)	0.03	(0.07)	.525	4.816	0.038	613.400
CD3%	51.57	(15.72)	55.07	(12.88)	52.33	(15.17)	.273	1.016	0.988	1.044
CD19%	9.42	(5.77)	9.28	(4.77)	9.39	(5.55)	.906	0.995	0.923	1.073
CD4%	40.09	(12.38)	43.15	(10.73)	40.74	(12.08)	.235	1.021	0.986	1.058
$CD8^{bright}$%	11.60	(4.82)	12.96	(5.60)	11.89	(5.00)	.213	1.053	0.971	1.143
$CD56^+CD16^+$%	9.31	(5.21)	11.18	(6.48)	9.72	(5.54)	.118	1.060	0.985	1.141
$CD56^+CD16^-$%	1.65	(1.26)	1.57	(0.83)	1.63	(1.17)	.748	0.940	0.645	1.371
$CD4^+CD25^+$%	11.56	(2.79)	12.20	(3.15)	11.70	(2.88)	.291	1.078	0.938	1.239
IFN-γ (PHA)	519.6	(771.7)	939.0	(1493.2)	609.5	(980.1)	.064	1.000	1.000	1.001
IL-4 (PHA)	5.65	(4.37)	6.55	(5.99)	5.84	(4.76)	.263	1.448	0.758	2.768
Six months of age										
WBC	10.78	(3.11)	11.23	(3.16)	10.86	(3.11)	.527	1.045	0.911	1.199
Eosinophils	371.1	(553.0)	567.5	(454.8)	404.7	(541.1)	.183	1.000	1.000	1.001
Basophils	55.86	(29.58)	61.31	(31.89)	56.79	(29.94)	.420	1.006	0.992	1.019
IgE	14.36	(23.46)	49.72	(61.12)	20.43	(35.39)	.001	1.022	1.010	1.035
T_H1%	2.07	(1.13)	2.11	(0.92)	2.08	(1.09)	.888	1.030	0.685	1.550
T_H2%	0.33	(0.19)	0.39	(0.28)	0.34	(0.21)	.247	3.325	0.434	25.467
T_C1%	7.15	(8.57)	6.76	(5.56)	7.08	(8.12)	.835	0.994	0.939	1.052
T_C2%	0.05	(0.17)	0.04	(0.07)	0.05	(0.16)	.654	0.414	0.009	19.459
CD3%	62.38	(12.50)	58.66	(14.56)	61.74	(12.89)	.204	0.979	0.949	1.011
CD19%	14.43	(9.19)	15.76	(9.52)	14.65	(9.22)	.520	1.015	0.969	1.064
CD4%	44.47	(10.44)	41.82	(10.53)	44.02	(10.47)	.260	0.976	0.935	1.018
$CD8^{bright}$%	13.76	(5.27)	12.68	(3.51)	13.58	(5.02)	.336	0.954	0.867	1.050
$CD56^+CD16^+$%	6.86	(4.46)	6.35	(4.95)	6.77	(4.53)	.614	0.974	0.878	1.080
$CD56^+CD16^-$%	0.98	(1.14)	0.86	(0.56)	0.96	(1.06)	.647	0.839	0.397	1.777
$CD4^+CD25^+$%	10.26	(2.22)	10.98	(2.18)	10.39	(2.22)	.154	1.155	0.947	1.408
IFN-γ (PHA)	3148.0	(3480.5)	1935.2	(2552.4)	2951.8	(3369.5)	.124	1.000	1.000	1.000
IL-4 (PHA)	13.20	(11.90)	13.70	(9.25)	13.28	(11.48)	.056	0.472	0.218	1.020

Abbreviations: IFN, interferon; Ig, immunoglobulin; IL, interleukin; PHA, phytohemagglutinin; WBC, white blood cells.

Risk Factors for Atopic Dermatitis at 14 Months of Age

We analyzed whether immunological markers in cord blood could be risk factors for 14MAD(+). However, no significant differences were found in any of the immunological markers of cord blood between 14MAD(+) and 14MAD(–) (Table 4).

We also analyzed whether immunological markers at 6 months of age could be a risk factor for 14MAD(+). According to univariate logistic regression analysis, an increase in total IgE levels was associated with 14MAD(+) (Table 4). Risk also significantly increased among participants who were sensitized to egg white, milk, wheat, or dog dander at 6 months of age (Table 5).

After stepwise multivariate logistic regression, total IgE at 6 months of age (aOR, 1.018; 95% CI, 1.002-1.034; *P*=.030) and egg white–specific IgE (aOR, 23.246; 95% CI, 2.801-192.905; *P*=.004) remained in the model (Table 6).

A ROC curve analysis performed to evaluate the predictability of total IgE level at 6 months of age for distinguishing 6MAD(+) from 6MAD(–) revealed the AUC of the total IgE levels to be 0.726 (95% CI, 0.607-0.845; *P*=.001). Since sensitization to egg white is not a continuous value, a ROC curve analysis was not performed. Hence, total IgE levels at 6 months of age were not only risk factors, but also predictors, for AD at 14 months of age.

Risk Factors for Recurrent Wheezing at 14 Months of Age

We analyzed whether immunological markers in cord blood could be risk factors for 14MRW(+). However, no significant differences were observed between 14MRW(+) and 14MRW(–) in any markers (Table 7).

We also analyzed whether immunological markers at 6 months of age could be risk factors for 14MRW(+). Using

Table 5. Odds Ratio (OR) for Having Atopic Dermatitis (AD) at 14 Months of Age According to Univariate Logistic Regression Analysis of Markers at 6 Months

		AD 14M (–)		AD 14M (+)				95% CI for OR	
			(n/total)		(n/total)	*P* Value	OR	Lower	Upper
Six months of age									
Egg white	≥ class 1	31.90%	(37/116)	87.50%	(21/24)	<.001	14.946	4.192	53.282
Cow's milk	≥ class 1	6.90%	(8/116)	37.50%	(9/24)	<.001	8.100	2.710	24.209
Wheat	≥ class 1	4.65%	(4/86)	33.33%	(5/15)	.002	10.250	2.358	44.561
Soy	≥ class 1	0%	(0/116)	4.17%	(1/24)	1.000	8.148×10^{9}	–	–
Dog dander	≥ class 1	6.03%	(7/116)	25.00%	(6/24)	.007	5.190	1.565	17.216
Cat dander	≥ class 1	1.72%	(2/116)	4.17%	(1/24)	.466	2.478	0.216	28.487
Df	≥ class 1	0.86%	(1/116)	8.33%	(2/24)	.060	10.455	0.908	120.354

Abbreviations: Df, *Dermatophagoides farinae*.

Table 6. Adjusted Odds Ratio (aOR) for Having Atopic Dermatitis at 14 Months of Age According to Multivariate Logistic Regression Analysis of Markers at 6 Months

				95% CI for aOR	
		P Value	aOR	Lower	Upper
Six months of age					
Step 1	IgE	.125	1.020	0.995	1.045
	Egg white ≥ class 1	.005	21.706	2.489	189.321
	Cow's milk ≥ class 1	.636	0.539	0.042	6.964
	Wheat ≥ class 1	.933	1.094	0.135	8.888
	Dog dander ≥ class 1	.215	3.316	0.499	22.038
Step 2	IgE	.105	1.020	0.996	1.044
	Egg white ≥ class 1	.004	22.072	2.617	186.170
	Cow's milk ≥ class 1	.639	0.555	0.047	6.527
	Dog dander ≥ class 1	.205	3.358	0.517	21.828
Step 3	IgE	.057	1.015	1.000	1.032
	Egg white ≥ class 1	.005	20.921	2.522	173.568
	Dog dander ≥ class 1	.222	3.100	0.503	19.088
Step 4	IgE	.030	1.018	1.002	1.034
	Egg white class ≥1	.004	23.246	2.801	192.905

Abbreviations: Ig, immunoglobulin.